© 2016. Published by The Company of Biologists Ltd | Development (2016) 143, 318-328 doi:10.1242/dev.127860

RESEARCH ARTICLE

Prox1 and fibroblast growth factor receptors form a novel regulatory loop controlling lens fiber differentiation and gene expression

Dylan S. Audette[1], Deepti Anand[1], Tammy So[2], Troy B. Rubenstein[1], Salil A. Lachke[1,3], Frank J. Lovicu[2] and Melinda K. Duncan[1,*]

ABSTRACT

Lens epithelial cells differentiate into lens fibers (LFs) in response to a fibroblast growth factor (FGF) gradient. This cell fate decision requires the transcription factor Prox1, which has been hypothesized to promote cell cycle exit in differentiating LF cells. However, we find that conditional deletion of *Prox1* from mouse lenses results in a failure in LF differentiation despite maintenance of normal cell cycle exit. Instead, RNA-seq demonstrated that Prox1 functions as a global regulator of LF cell gene expression. Intriguingly, Prox1 also controls the expression of fibroblast growth factor receptors (FGFRs) and can bind to their promoters, correlating with decreased downstream signaling through MAPK and AKT in *Prox1* mutant lenses. Further, culturing rat lens explants in FGF increased their expression of Prox1, and this was attenuated by the addition of inhibitors of MAPK. Together, these results describe a novel feedback loop required for lens differentiation and morphogenesis, whereby Prox1 and FGFR signaling interact to mediate LF differentiation in response to FGF.

KEY WORDS: Lens, Morphogenesis, Regulatory loop

INTRODUCTION

Tissue morphogenesis requires cell-cell communication, often mediated by growth factors, that reprograms cellular phenotypes. This response is fine-tuned by regulation of growth factor receptor expression, allowing cells to respond to, or ignore, specific stimuli (Cross and Dexter, 1991; Scata et al., 1999). These processes can be studied in the ocular lens as cells differentiate in response to growth factor signaling, and the simplicity of this tissue makes it an ideal model with which to study the resulting morphological and molecular changes (Lovicu et al., 2011).

The lens arises from an area of head ectoderm termed the lens placode, which invaginates to form the lens vesicle (LV) (Streit, 2004). The anterior hemisphere of the LV retains its epithelial morphology, while the posterior cells extend anteriorly and terminally differentiate into primary lens fibers (LFs) (Bhat, 2001). This process requires fibroblast growth factor (FGF), which is secreted by the developing retina and binds to fibroblast growth factor receptors (FGFRs) expressed by lens cells (de Iongh and Duncan, 2015; Lovicu et al., 2011). Although FGFRs are required for LF differentiation (Zhao et al., 2008) and are upregulated in differentiating LFs (de Iongh et al., 1997), the regulation of these receptors remains undefined.

LF differentiation also requires the transcription factors cMaf (Kim et al., 1999), Sox1 (Nishiguchi et al., 1998) and Prox1 (Wigle et al., 1999), as mice mutant for any of these genes never form LFs. Prox1 is a sequence-specific DNA-binding transcription factor that is defined by its conserved, atypical homeodomain (Chen et al., 2008; Tomarev et al., 1996). Although Prox1 is first detected in the lens placode (Duncan et al., 2002), eyes lacking Prox1 develop normally until the posterior LV cells fail to elongate into LFs (Wigle et al., 1999). Although it has been proposed that Prox1 regulation of cell cycle exit drives this phenotype (Wigle et al., 1999), other mutants with cell cycle exit defects do not phenocopy the *Prox1* null lens (Fromm et al., 1994; Zhang et al., 1998). Here, we further investigate the cause of the LF cell morphogenesis failure observed in *Prox1* mutant mice.

RESULTS

Mice with lens-specific deletion of *Prox1* phenocopy the lens morphology of *Prox1* null mice

As *Prox1* null mice die *in utero* (Wigle and Oliver, 1999), $Prox1^{flox/flox}$*MLR10Cre+* (*Prox1* cKO) mice were generated that inactivate *Prox1* in lens. *Prox1* cKO lenses develop normally prior to E11.5; however, whereas the primary LFs of wild-type (WT) mice elongate by E12.5 (Fig. 1A) and stain vibrantly with Eosin, this does not occur in *Prox1* cKO lenses (Fig. 1D). Secondary LF differentiation begins in WT by E13.5 (Fig. 1B,C). By contrast, most *Prox1* cKO lenses do not exhibit LF elongation and never stain intensely with Eosin (Fig. 1E,F).

Prox1 protein is located in the nuclei of differentiating LFs at E12.5 (Fig. 1G) and is maintained at the transition zone of E13.5 and E15.5 WT lenses (Fig. 1H,I). Prox1 protein levels are unaltered at E11.5 in *Prox1* cKO LV (not shown), are substantially reduced at the posterior of *Prox1* cKO lenses by E12.5 (Fig. 1J), and are below the limit of detection at E13.5 and E15.5 (Fig. 1K,L).

Prox1 cKO LFs exit the cell cycle appropriately and do not undergo robust apoptosis

Since *Prox1* mutant lens phenotypes have been hypothesized to result from cell cycle exit failure in the posterior LV (Wigle et al., 1999), we evaluated DNA synthesis and cell cycle exit. In WT mice, cells undergoing DNA synthesis are confined to the lens epithelium at E13.5 (Fig. 2A,A′). Similarly, only the most anterior cells of *Prox1* cKO LVs exhibit detectable DNA synthesis (Fig. 2B,B′). Cell cycle exit coincident with LF cell differentiation is preceded by elevated expression of the cell cycle inhibitors (CKIs) $p27^{Kip1}$ and $p57^{Kip2}$ (Cdkn1b and Cdkn1c – Mouse Genome Informatics)

[1]Department of Biological Sciences, University of Delaware, Newark, DE 19716, USA. [2]Discipline of Anatomy & Histology, Bosch Institute & Save Sight Institute, University of Sydney, Sydney, New South Wales 2000, Australia. [3]Center for Bioinformatics and Computational Biology, University of Delaware, Newark, DE 19716, USA.

*Author for correspondence (duncanm@udel.edu)

Received 7 July 2015; Accepted 26 November 2015

Development (2016) 143, 318-328 doi:10.1242/dev.127860

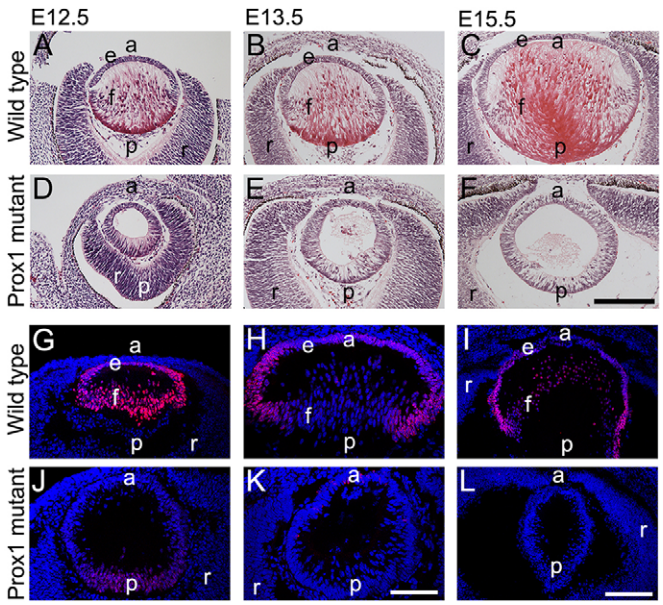

Fig. 1. *Prox1* deletion from the early lens arrests its development at the LV. (A-F) Mouse eye sections at E12.5 (A,D), E13.5 (B,E) and E15.5 (C,F) stained with Hematoxylin and Eosin. In WT, primary lens fibers (LFs; pink) were evident by E12.5 (A), with secondary fibers produced at E13.5 (B) and E15.5 (C). In *Prox1* cKO lenses, the posterior-most cells never elongate into eosinophilic primary (D) or secondary fibers (E,F). (G-L) Immunofluorescence staining for Prox1. Prox1 is expressed in WT primary LFs at E12.5 (G) and in elongating secondary LFs at E13.5 (H) and E15.5 (I). Prox1 protein levels are reduced in *Prox1* cKO by E12.5 (J), and Prox1 immunoreactivity is absent from *Prox1* cKO lenses by E13.5 (K,L). (A-F) Blue, Hematoxylin; pink, Eosin. (G-L) Blue, Draq5 (DNA); red, Prox1. a, anterior; p, posterior; r, retina; e, lens epithelium; f, LFs. Scale bars: 200 µm in A-F; 100 µm in G-L.

(Zhang et al., 1998). WT lenses express $p27^{Kip1}$ (not shown) and $p57^{Kip2}$ (Fig. 2C,C′) in differentiating LFs at E13.5, and a similar pattern was detected in the E13.5 *Prox1* cKO LV (not shown; Fig. 2D,D′).

WT E13.5 lenses exhibit little to no programmed cell death as measured by TUNEL (Fig. 2E,E′). *Prox1* cKO contained a few TUNEL-positive nuclei at E13.5 (Fig. 2F,F′). The vasculature surrounding WT lenses had few or no TUNEL-positive nuclei at E13.5 (Fig. 2E,E″), whereas *Prox1* cKO eyes exhibited apoptosis of the lens vasculature at E13.5 (Fig. 2F,F′), leading to its loss by E15.5 (Fig. 1F).

Prox1 cKO mice have reduced expression of LF cell markers

The morphological changes occurring during LF cell differentiation are coincident with a huge increase in crystallin expression (Duncan et al., 2004). Notably, mRNA levels of all crystallin genes assayed were significantly downregulated in *Prox1* cKO lenses compared with WT (Fig. 3A). Immunostaining using pan-specific β-crystallin (Fig. 3B) and γ-crystallin (Fig. 3C) antibodies revealed prominent LF-specific protein expression in WT lenses, whereas immunoreactivity was absent in *Prox1* cKO lenses (Fig. 3E,F). Further, the levels of aquaporin 0 (Mip – Mouse Genome Informatics), the most abundant LF membrane protein (Fig. 3D) (Bassnett et al., 2009), were reduced at the mRNA (Fig. 3A) and protein (Fig. 3G) levels in *Prox1* cKO compared with WT (Fig. 3D).

Prox1 cKO presumptive LFs appropriately decrease expression of lens epithelial markers

The expression of lens epithelial cell markers in the posterior LV is decreased as it initiates LF differentiation (Hawse et al., 2005).

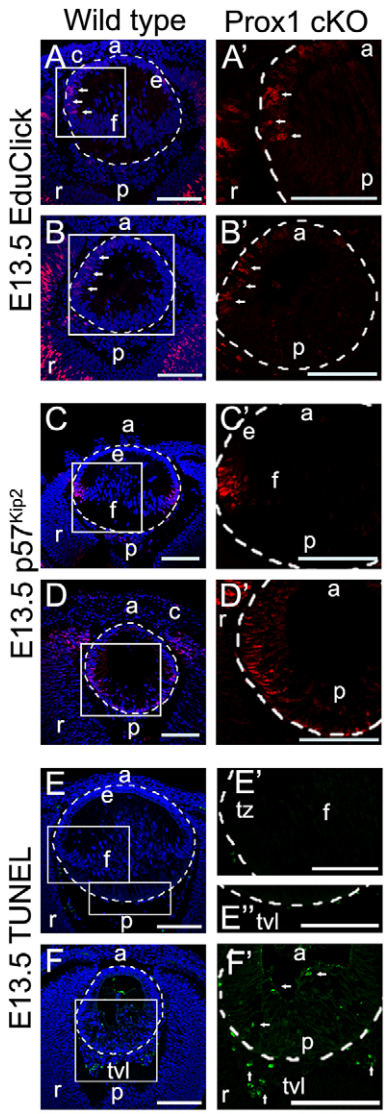

Fig. 2. Posterior cells of the *Prox1* cKO LV exit the cell cycle. (A,A′) E13.5 WT lenses exhibit EduClick (EduC)-positive cells (red) in the epithelium (arrows), but they were absent from the transition zone and from LFs. (B,B′) E13.5 *Prox1* cKO lenses maintained cell proliferation in the anterior aspect of the lens (arrows), while no EduC labeling was detected at the lens posterior. (C,C′) Immunofluorescence staining of WT E13.5 lenses showed expression of the cell cycle inhibitor $p57^{Kip2}$ (red) in differentiating LFs. (D,D′) Similarly, $p57^{Kip2}$ was still expressed in the most posterior cells of the *Prox1* cKO lens. (E-F′) TUNEL assays. Programmed cell death was not observed in WT lenses or the tunica vasculosa lentis at E13.5 (E,E′). Isolated TUNEL-positive nuclei were seen in the posterior LV of *Prox1* cKO at E13.5 (F,F′, arrows); however, robust TUNEL staining was consistently observed in the tunica vasculosa lentis of *Prox1* cKO at E13.5 (F,F′, arrows). Boxed regions in A-F are shown at higher magnification in A′-F′. The dashed line delineates the lens capsule. (A-F′) Blue, Draq5 (DNA). (A-B′) Red, EduC. (C-D′) Red, $p57^{Kip2}$. (E-F′) Green, TUNEL. a, anterior eye; p, posterior eye; r, retina; c, cornea; e, lens epithelium; tvl, tunica vasculosa lentis; f, LFs. Scale bars: 100 µm.

E-cadherin (cadherin 1) protein is restricted to the epithelium of E14.5 WT lenses (Fig. 4A), and this distribution is maintained in *Prox1* cKO lenses (Fig. 4B). The transcription factor Pax6 is abundant in the LV and lens epithelium (Fig. 4C), with lower levels present in LFs (Shaham et al., 2009). The highest Pax6 levels are restricted to the anterior cells of the *Prox1* cKO lens (Fig. 4D).

Development (2016) 143, 318-328 doi:10.1242/dev.127860

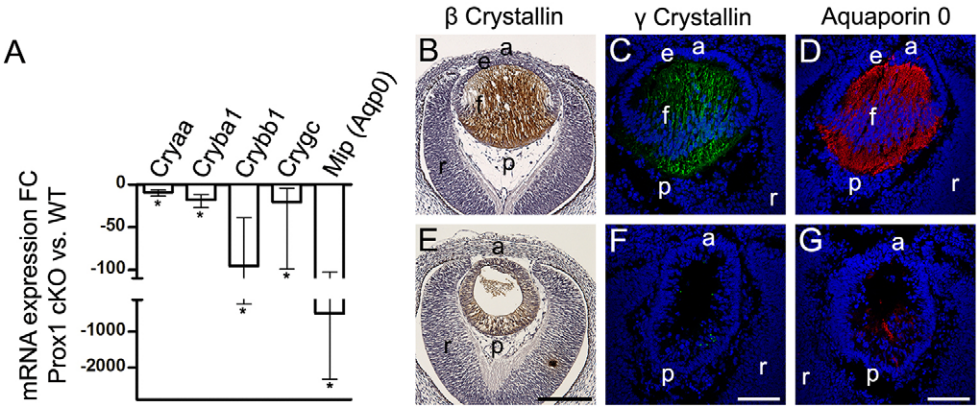

Fig. 3. LF marker expression decreases in *Prox1* cKO. (A) qRT-PCR of E14.5 *Prox1* cKO lenses compared with WT. *$P \leq 0.01$ by nested ANOVA. αA-crystallin (*Cryaa*; $P=0.007$), βA1-crystallin (*Cryba1*; $P=0.001$), βB1-crystallin (*Crybb1*; $P=0.002$), γC-crystallin (*Crygc*; $P=0.0001$) and aquaporin 0 ($P=0.004$) mRNA levels are reduced in *Prox1* cKO lenses. Error bars indicate s.d.; $n=3$. (B,E) β-crystallin protein (brown) localizes to WT LFs at E13.5 (B), but this is reduced in *Prox1* cKO lenses (E). (C,F) γ-Crystallin protein (green) is found in elongated LFs in the E13.5 WT lens (C), but its levels are reduced in the *Prox1* cKO lens (F). (D,G) Aquaporin 0 protein (red) is found in E13.5 WT LFs (D), whereas little is detected in *Prox1* cKO lenses (G). (B,E) Blue, Hematoxylin. (C,D,F,G) Blue, Draq5 (DNA). a, anterior eye; p, posterior eye; r, retina; e, lens epithelium; f, LFs. Scale bars: 200 µm in B,E; 100 µm in C,D,F,G.

Global gene expression profiling reveals that Prox1 is a major regulator of lens-enriched gene expression

RNA-seq was performed on E13.5 lenses to elucidate how the lens transcriptome is affected immediately following the loss of Prox1 protein expression (full data are available at GEO under accession GSE69940). Overall, 642 genes were differentially expressed in the E13.5 *Prox1* cKO lens; 356 were expressed at lower levels in *Prox1* cKO lenses [referred to as downregulated differentially expressed genes (downDEGs); Table S3], whereas 286 were elevated in *Prox1* cKO [upregulated differentially expressed genes (upDEGs); Table S4].

Analysis of downDEGs using DAVID (Huang et al., 2009) (Fig. 5A) revealed that the most significant gene ontology (GO) category was 'structural constituents of the eye lens', which included every crystallin known to be an LF cell marker in embryos (*Cryaa*, *Cryba1*, *Cryba2*, *Cryba4*, *Crybb1*, *Crybb3* and all gamma crystallins) as well as aquaporin 0. *Prox1* cKO downDEGs were also enriched in regulators of cytoskeletal organization as well as the LF-enriched, RNA granule-encoding genes *Tdrd7* (Lachke et al., 2011) and *Caprin2* (Dash et al., 2015). Notably absent were genes that regulate the cell cycle, consistent with our findings presented in Fig. 2.

The most enriched GO category of upDEGs (Fig. 5B) included genes involved in cell adhesion. Others included genes associated with non-LF cell lineages such as skeletal system development and melanin biosynthesis. Taken together, these data indicate that Prox1 turns off the expression of genes associated with non-lens lineages, while positively regulating the expression of effectors of LF morphogenesis and function.

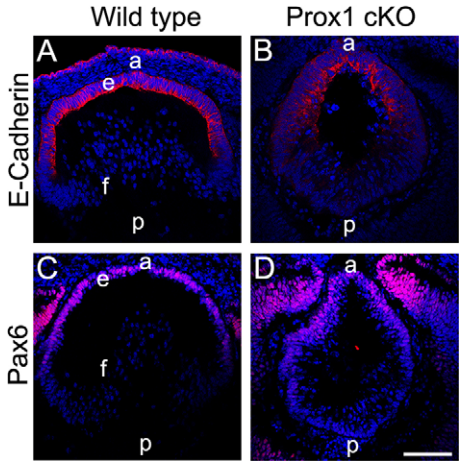

Fig. 4. *Prox1* cKO lenses have a normal distribution of epithelial markers. (A,B) E-cadherin (red) is expressed in the epithelium and absent at the transition zone of both WT (A) and *Prox1* cKO (B) E13.5 lenses. (C,D) The transcription factor Pax6 (red) is preferentially localized to the lens epithelium and reduced at the transition zones of both WT (C) and *Prox1* cKO (D) lenses at E14.5. Blue, Draq5 (DNA). a, anterior eye; p, posterior eye; e, lens epithelium; f, LFs. Scale bar: 100 µm.

A majority of genes downregulated in the *Prox1* cKO exhibit lens-enriched expression

DAVID categorizes differentially expressed genes (DEGs) into functionally related groups. However, it does not address the expression dynamics of DEGs in normal lens development – information that can provide additional insights into the significance of Prox1 in lens biology. Therefore, the effect of Prox1 on the expression of genes crucial for lens phenotype was determined by examining which DEGs are preferentially expressed in the lens using *iSyTE*, a tool that identifies genes with lens-enriched expression by ranking them based on a 'lens-enrichment score'. The lens-enrichment score for a gene is defined as the measure of its fold difference in expression between the lens and the whole embryonic body reference at $P<0.05$. Lens-enrichment scores change as lens differentiation proceeds from the lens pit at E10.5 to the early lens at E12.5, potentially indicating that a gene exhibits enriched expression in differentiating LFs (Lachke et al., 2012). Fig. 5C-H plots the fold change (FC) in expression between DEGs in *Prox1* cKO lenses against their *iSyTE* lens-enrichment scores. From the onset of LF differentiation at E12.5 through postnatal stages, most downDEGs were lens enriched; note the clustering of the *Prox1* cKO downDEGs in the upper left quadrant of Fig. 5E-H. By contrast, most upDEGs were not lens enriched, and this trend became more obvious following the onset of LF differentiation (see lower right quadrant of Fig. 5E-H). The lens-enrichment scores of the downDEGs were significantly higher than those of the upDEGs at all stages examined. However, this relationship was especially obvious after the onset of LF differentiation (E12.5) (Fig. 5E-H).

Further, comparison of the genes that *iSyTE* identified as 'most lens enriched' with the DEGs in *Prox1* cKO lenses demonstrated

Development (2016) 143, 318-328 doi:10.1242/dev.127860

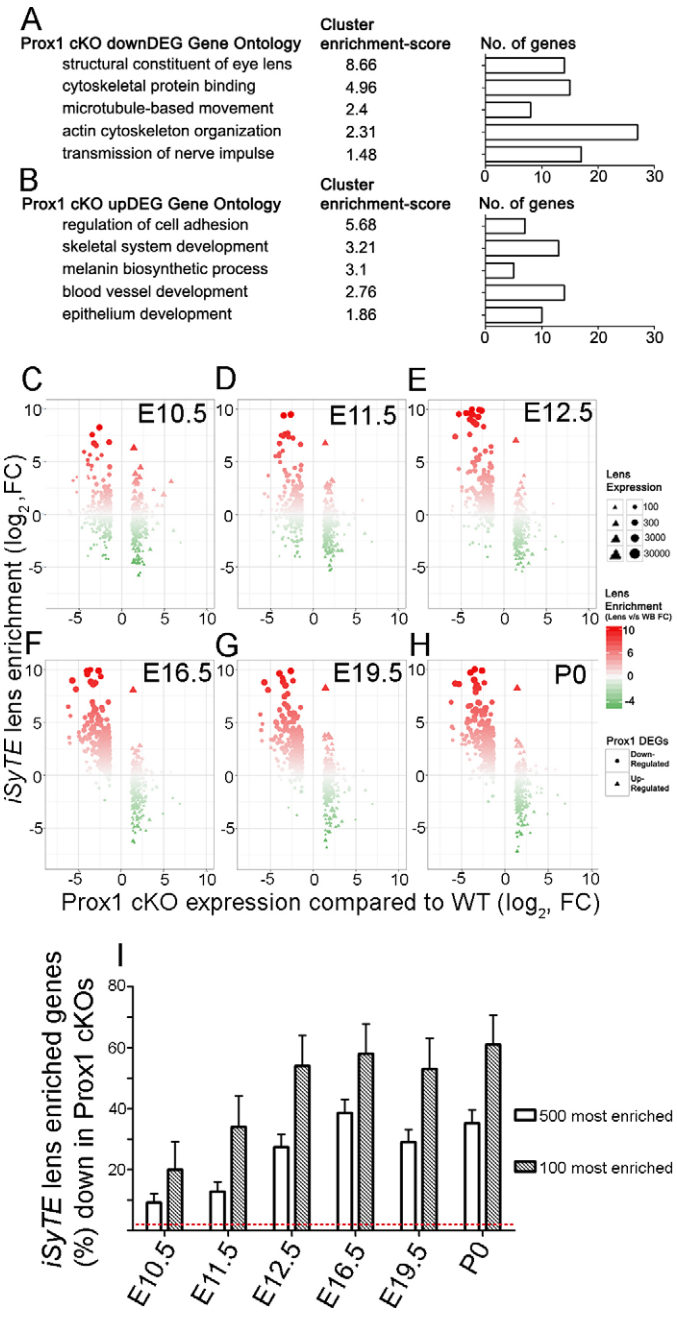

Fig. 5. *Prox1* deletion results in the misregulation of genes that are highly enriched in expression in the developing lens. RNA-seq was performed on E13.5 *Prox1* cKO and WT lenses immediately following the loss of Prox1 protein. (A,B) The DAVID bioinformatics resource was used to group/cluster the downregulated (downDEGs) (A) and upregulated (upDEGs) (B) genes into functionally related gene ontology (GOs) categories with cluster enrichment scores representing their likelihood of affecting biological function. (C-H) The relative lens-enrichment score of each DEG [FC, fold change from the whole body (WB) control] at E10.5 (C), E11.5 (D), E12.5 (E), E16.5 (F), E19.5 (G) and P0 (H) was determined using *iSyTE*. The values obtained were plotted in a dot plot with *Prox1* cKO DEGs [fold change (FC) of gene expression in *Prox1* cKO lens compared with WT control] on the *x*-axis. The *iSyTE* lens enrichment in expressed as FC compared with the WB reference dataset (as described by Lachke et al., 2012) on the *y*-axis. As shown in the key, the size of the solid circles (downregulated in *Prox1* cKO) or triangles (upregulated in *Prox1* cKO) represents the lens expression levels in microarray fluorescence intensity units (data obtained from *iSyTE* and other publically available datasets). The color of the circles or triangles represents lens-enrichment scores in FC (red, lens-enriched genes; green, genes expressed at higher levels in the WB reference). As the lens progresses from E12.5 to P0, the vast majority of DEGs in the downDEGs category fall into the lens-enriched (upper left quadrant) category compared with upDEGs (upper right quadrant), which was significant by a χ^2 test for goodness of fit (P<0.00001). Notably, χ^2 values increased between the LV and the onset of LF differentiation (see Materials and Methods). (I) The fraction of the top 500 or top 100 lens-enriched genes at various developmental stages that are downregulated in *Prox1* cKO. Error bars indicate s.e.m.; n=3. Red dotted line indicates the percentage of genes expected to be downregulated in a random sample.

that Prox1 is required for the expression of a significant, although relatively small, fraction of lens-enriched genes at E10.5 (LV). However, as LF differentiation begins at E12.5, the requirement for Prox1 in regulating the lens developmental program increases dramatically (Fig. 5I). Prox1 was required for the expression of 54% of the top 100 most lens-enriched genes at E12.5, a figure that increased to 60% during secondary LF differentiation (Fig. 5I). A χ^2 test for goodness of fit found this to differ significantly from random chance (P<0.0001, two-tailed t-test).

These data support the idea that Prox1 plays major roles in regulating the gene expression that confers the LF cell phenotype.

FGFR expression decreases in *Prox1* mutants

As none of the *Prox1* cKO DEGs included known transcriptional regulators of LF cell differentiation (Tables S3 and S4), *Prox1* cKO DEGs were searched for genes involved in regulatory loops known to control LF fate. FGF regulates LF differentiation by binding to transmembrane FGF receptors (FGFRs) on lens cells (Lovicu and McAvoy, 2005), and the simultaneous removal of *Fgfr1*, *Fgfr2* and *Fgfr3* results in a failure of LF differentiation similar to the *Prox1* cKO phenotype (Zhao et al., 2008). Notably, *Fgfr3* mRNA levels decreased 10-fold in the lens following Prox1 loss, whereas *Fgfr1* and *Fgfr2* were unchanged (Table 1). This was validated in E14.5 WT and *Prox1* cKO lenses by qRT-PCR (Fig. 6A).

Interestingly, RNA-seq identified two additional genes that could regulate FGF signaling in the lens. FGF receptor-like 1 (*Fgfrl1* or *Fgfr5*) is the most abundant FGFR mRNA in the E13.5 lens, and its levels are 4-fold reduced in *Prox1* cKO lenses (Table 1). Lactase-like (*Lctl*, klotho γ or *Klph*) was the most profoundly downregulated

Table 1. FGF receptor and co-receptor mRNA levels in *Prox1* cKO versus WT lenses determined by RNA-seq

FGFR and FGF co-receptor expression from *Prox1* cKO versus WT RNA-seq

Gene symbol	Gene description	WT RPKM	FC
FGFR gene expression			
Fgfr1	Fibroblast growth factor receptor 1	15	−1.14
Fgfr2	Fibroblast growth factor receptor 2	13.4	−1.23
Fgfr3	Fibroblast growth factor receptor 3	23.9	−10.8
Fgfr4	Fibroblast growth factor receptor 4	0.095	1
Fgfrl1 (*Fgfr5*)	Fibroblast growth factor receptor-like 1	32.3	−4.2
Klotho gene expression			
Lctl	Lactase-like (klotho gamma)	2.34	−234
Kl	Klotho	0.002	1
Klb	Klotho beta	0.051	1

The mean transcript abundance for each FGFR is given in reads per million per kilobase (RPKM). Differential gene expression between WT and *Prox1* cKO lenses is represented by fold change (FC).

Development (2016) 143, 318-328 doi:10.1242/dev.127860

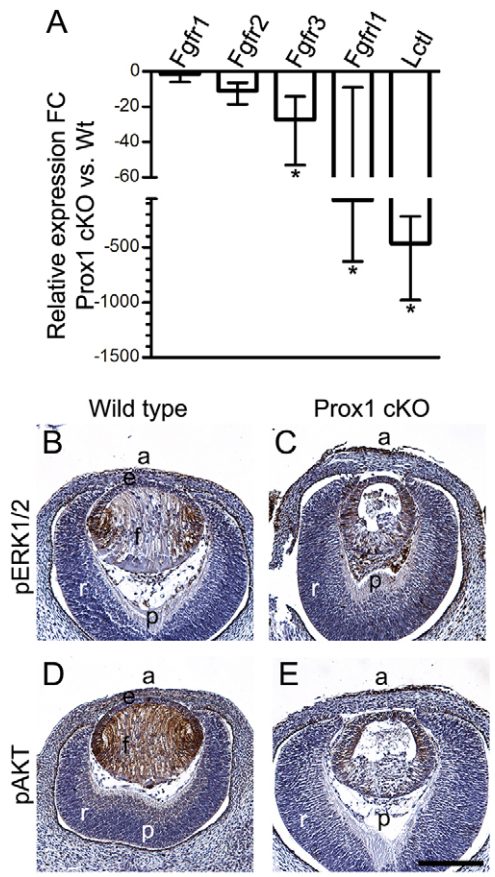

Fig. 6. *Prox1* cKO lenses exhibit a decrease in the expression of three FGFRs and their downstream signaling. (A) qRT-PCR revealed significant decreases in the expression of *Fgfr3* (P=0.01), the atypical receptor *Fgfrl1* (P=0.04), and the FGF co-receptor *Lctl* (P=0.03) in E14.5 *Prox1* cKO lenses; *P<0.05 by nested ANOVA. Error bars indicate s.d.; n=3. (B) By immunohistochemistry pErk1/2 (brown) was detected at the transition zones of WT lenses (B) and was absent from the equator of *Prox1* cKO lenses (C) at E13.5. Similarly, robust pAKT staining (brown) was observed at the transition zones of WT lenses at E13.5 (D), but was absent in the posterior LFs of *Prox1* cKO lenses (E). Blue, Hematoxylin. a, anterior; p, posterior, r, retina; e, epithelium; f, LFs. Scale bar: 100 µm.

gene following Prox1 loss and is the only Klotho family member expressed in the lens (Table 1). The downregulation of these genes was confirmed and found to be even more profound at E14.5 by qRT-PCR (Fig. 6A).

Prox1 cKO lenses exhibit reduced MAPK and AKT activation

Since *Prox1* deletion led to significant reductions in FGFR mRNA levels in the lens, we next determined if these changes resulted in decreased FGFR-mediated signal transduction. Ligand association with FGFRs initiates signaling through MAPK and PI3K/AKT pathways to stimulate LF differentiation (Wang et al., 2009). Phosphorylated (p) Erk1/2 (Mapk3/1; MAPK effector) was found at the WT transition zone (Fig. 6B), whereas *Prox1* cKO lenses exhibited less active Erk1/2 at the lens equator, although apparently normal levels of the pErk1/2 were observed in the lens epithelium (Fig. 6C). pAKT is detected in the differentiating LFs of E14.5 WT lenses (Fig. 6D). By contrast, AKT phosphorylation was decreased in the presumptive LFs of *Prox1* cKO mice (Fig. 6E), although pAKT levels appeared unaffected in the anterior-most lens cells. These data suggest that decreased FGFR expression in *Prox1* cKO lenses decreases FGFR-mediated signal transduction.

Putative Prox1 binding sites in *Fgfr3*, *Fgfrl1* and *Lctl* are evolutionarily conserved and Prox1 binds to these genes in the lens *in vivo*

Since FGFR expression and signaling are attenuated in the *Prox1* cKO lens, the potential for Prox1 to directly bind to the FGFR promoters was assessed. The regions upstream of the transcriptional start site (TSS) of the human, mouse and chicken *Fgfr3*, *Lctl* and *Fgfrl1* genes were searched for the three previously described Prox1 binding motifs (Chen et al., 2008). These genes were then aligned, revealing that several predicted Prox1 binding sites are evolutionarily conserved in the putative *Fgfr3* (Fig. 7A), *Fgfrl1* (Fig. 7B), *Lctl* (Fig. 7C) promoters. Chromatin immunoprecipitation (ChIP) was performed on chicken embryonic lenses and revealed that Prox1 is likely to bind upstream of the TSS of all three genes, as measured by statistically significant enrichment of fragment recoveries compared with a region 5 kb downstream of the putative TSS (Fig. 7D-F). One caveat to this conclusion is that the chicken *LCTL* gene annotation was only provisional. These data are consistent with the prior identification of evolutionarily conserved Prox1 binding sites in the *FGFR3* promoter, and the ability of Prox1 to bind to these sites in electrophoretic mobility shift assays (Shin et al., 2006).

Prox1 expression is regulated by FGFR signaling

Prox1 protein levels increase sharply coincident with LF differentiation (Fig. 1I-K) (Duncan et al., 2002), and mice lacking Fgfr1-3 from the lens downregulate Prox1 protein levels (Zhao et al., 2008), suggesting that FGF signaling regulates Prox1 levels in the lens. Rat lens epithelial explants were cultured in a high dose of FGF, which promotes LF-like differentiation and morphology (McAvoy and Chamberlain, 1989). Although the explants cultured without FGF survived (Fig. 8A-C), only explants cultured with a differentiating dose of FGF (Fig. 8D-F) exhibited robust Prox1 expression (Fig. 8F). Further, when explants were cultured with a high dose of FGF and either an antagonist of FGFR signaling (Fig. 8G-I) or an inhibitor of the MAPK pathway effector Mek1 (Map2k1) (Fig. 8J-L), nuclear Prox1 levels were attenuated (Fig. 8I,L). Western blot analysis confirmed the upregulation of Prox1 expression in rat lens explants in response to FGF and the attenuation of this response by a MAPK inhibitor (Fig. 8M,N). Notably, inhibition of PI3K/AKT signaling did not affect Prox1 upregulation in response to FGF (Fig. 8M,N). These data suggest that the dramatic increase in Prox1 protein at the onset of LF differentiation is regulated by FGF signaling through FGFRs in a largely MAPK-mediated pathway.

DISCUSSION

Prior to this work, Prox1 function in lens development was understudied. Prox1 expression was known to correlate with LF differentiation (Duncan et al., 2002) and to be required for LF morphogenesis (Wigle et al., 1999), but, whereas *in vitro* experiments suggested that Prox1 regulates the expression of LF differentiation markers (Chen et al., 2008; Lengler et al., 2001), this was not supported by the only *in vivo* investigation performed on Prox1 function in lens (Wigle et al., 1999). In the present study we sought to expand our understanding of the mechanisms by which Prox1 mediates LF differentiation.

Prox1 is not a major regulator of cell cycle exit after LV closure

Prior work on *Prox1* null mice demonstrated that the lens is arrested at the LV stage, indicating an essential role of Prox1 in LF cell morphogenesis. It was proposed that Prox1 generates LV

Development (2016) 143, 318-328 doi:10.1242/dev.127860

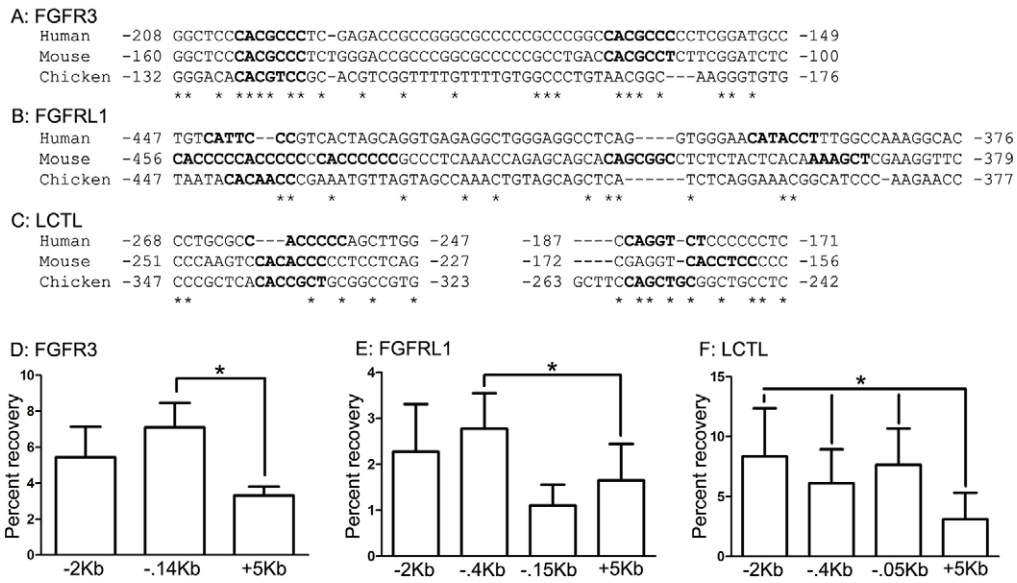

Fig. 7. Prox1 binds to the putative *FGFR3*, *FGFRL1* and *LCTL* promoters as assayed by ChIP. (A-C) The regions upstream of the transcriptional start site (TSS) of *Fgfr3*, *Fgfrl1* and *Lctl* were screened for matches to the Prox1 consensus binding sequences: (A or C) AAG(N)(not A) or CA(not A)(N)(N)(C or G)(C or T) (Chen et al., 2008). Putative Prox1 binding sites (bold) were identified in the *Fgfr3* promoters of human, mouse and chicken (A), which matched the previously characterized Prox1 binding sites in the human *FGFR3* promoter (Shin et al., 2006) and are numbered relative to the TSS. Predicted Prox1 binding sites (bold) are present upstream of human, mouse and chicken *Fgfrl1* (B) and *Lctl* (C) putative TSSs. (D-F) ChIP was performed on embryonic chicken lenses, pulling down chromatin complexed with Prox1 protein. DNA fragments corresponding to the regions upstream of *FGFR3* (D), *FGFRL1* (E) and *LCTL* (F) were recovered at an enriched frequency when compared with regions 5 kb downstream of each TSS, as assayed by qRT-PCR followed by two-way ANOVA with $*P \leq 0.05$. Error bars indicate s.d.; $n=3$.

polarity by downregulating the expression of E-cadherin in the posterior LV and upregulating expression of the cell cycle inhibitors $p27^{Kip1}$ and $p57^{Kip2}$ (Wigle et al., 1999). By contrast, although *Prox1* cKO lenses in the present study exhibited morphological similarities to *Prox1* null lenses, they differed at the molecular level. In *Prox1* cKO lenses, E-cadherin was restricted to the anterior LV (Fig. 4B), while $p27^{Kip1}$ and $p57^{Kip2}$ expression was maintained posterior to the lens equator (not shown; Fig. 2D,D′). This difference in phenotype is likely to be derived from the timing of Prox1 loss, as the *Prox1* cKO lenses do not lose all Prox1 protein until after LV closure (Fig. 1K), whereas Prox1 was absent from all tissues in the prior report (Wigle et al., 1999). The observation that a lack of cell cycle exit is insufficient to explain the *Prox1* null lens phenotype is consistent with prior reports of retinoblastoma mutant (Fromm et al., 1994; Pan and Griep, 1994) and $p27^{Kip1-/-};p57^{Kip2+/-}$ (Zhang et al., 1998) lenses, which do not phenocopy the morphology of lenses lacking Prox1, despite maintaining cell proliferation in the posterior lens.

Prox1 is a major regulator of LF cell-enriched gene expression

Prox1 cKO lenses exhibited decreased levels of every LF marker that was assayed by immunolocalization and qRT-PCR (Fig. 3). Then, RNA-seq was performed on *Prox1* cKO lenses as an unbiased approach to discover potential pathways regulated by Prox1 in the lens. DAVID-based analysis of DEGs showed that many downDEGs have a known function in the lens. On the other hand, *iSyTE* allowed an appreciation of the dynamic expression of all DEGs in normal lens development. Specifically, the analysis of *Prox1* cKO DEGs by *iSyTE* suggests that *Prox1* cKO downDEGs are normally upregulated in expression during LF differentiation. Further, these data suggest that Prox1 is required for the expression of 60% of genes exhibiting the most highly lens-enriched expression pattern at these developmental time points (Fig. 5).

Although these findings contrast with a prior report that suggested that Prox1 had no significant role in lens marker expression, this is likely to be due to the non-quantitative nature of that study (Wigle et al., 1999). Notably, prior ChIP analyses show that the βB1-crystallin locus (downregulated 7-fold in E13.5 *Prox1* cKO lens as assessed by RNA-seq; 95-fold in E14.5 *Prox1* cKO lens as assessed by qRT-PCR, see Fig. 3) is bound by Prox1 in lens chromatin (Chen et al., 2008), while co-transfection analyses show that both the βB1-crystallin (Chen et al., 2008; Cui et al., 2004) and γF-crystallin (downregulated 44-fold in the E13.5 *Prox1* cKO lens) (Lengler et al., 2001) promoters have functional Prox1 binding sites. Together, these data support the idea that Prox1 directly regulates at least a subset of genes that express markers of LF cell differentiation.

Prox1 cKO downDEGs may shed light on the molecular mechanisms underlying LF morphogenesis

Differentiating LFs undergo massive morphological changes, which include cytoskeleton rearrangements that are required for LF elongation. DAVID analysis of the *Prox1* cKO DEGs suggested that Prox1 regulates this process. As lens epithelial cells differentiate into LF cells, they dismantle actin stress fibers in response to PI3K/AKT signaling (Weber and Menko, 2006b) and repolymerize them into cortical actin bundles that reside under the LF cell plasma membrane (Weber and Menko, 2006a). Notably, the *Prox1* cKO downDEGs include numerous genes that could regulate actin (Fig. 5A) and therefore might be involved in this process. The ultimate lack of LF cell elongation could result from both the loss of fiber cell-enriched actin regulators and the attenuation of AKT signaling (Fig. 6E) observed in *Prox1* cKO lenses.

Elongating LFs also require microtubules, as the culture of lens cells in inhibitors of microtubule polymerization or monomer association significantly decreases LF elongation (Piatigorsky, 1975). The *Prox1* cKO downDEGs include several genes that may regulate microtubule dynamics, including tubulin itself, as well

Development (2016) 143, 318-328 doi:10.1242/dev.127860

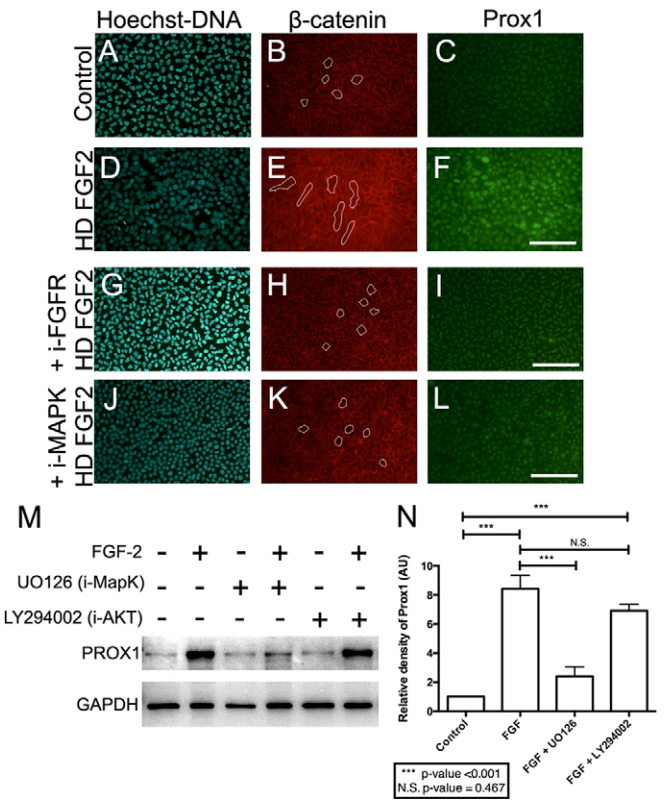

Fig. 8. Prox1 expression is regulated by FGFR-mediated MAPK signaling. (A-C) Explants cultured without FGF2 maintained their cuboidal epithelial morphology (B, cell outlines) and did not upregulate Prox1 (C). (D-F) Explants cultured in a high dose (100 ng/ml) of FGF2 displayed cell multi-layering and cell elongation (E, cell outlines), features of LF differentiation *in vitro*, and exhibited elevated levels of nuclear Prox1 (F). (G-I) When cultured in the presence of the FGFR antagonist SU5402, explants maintained their cuboidal epithelial morphology (H, cell outlines) and did not increase their nuclear Prox1 expression (I) in response to FGF2, similar to controls not treated with FGF2 (C). (J-L) When cultured in the presence of an inhibitor of the MAPK pathway kinase Mek1 (UO126), explants maintained their cuboidal epithelial morphology (K, cell outlines) and slightly increased their nuclear Prox1 expression (L) in response to FGF2, as compared with controls not treated with FGF2 (C); however, these explants did not recapitulate the upregulation of nuclear Prox1 observed in non-inhibited samples (F). (M,N) Explants cultured with or without (100 ng/ml) FGF2 and with or without inhibitors were analyzed by western blot for Prox1 and Gapdh. Blots were quantified by densitometry using ANOVA followed by a Šídák multiple comparison post-test and are presented with s.e.m. Induction of LF differentiation with FGF2 resulted in a significant upregulation of Prox1 that was blocked by addition of the MAPK inhibitor UO126 but not significantly blocked by addition of the PI3K/AKT inhibitor LY294002. Blue, Hoechst; red, β-catenin; green, Prox1. Scale bars: 100 µm.

as other tubulin-interacting proteins. Further, the downDEGs include regulators of transport along microtubule bundles, which may traffic materials required for LF elongation. Overall, these data suggest that Prox1 plays a major role in modulating the cytoskeletal dynamics in the lens that is required for LF elongation.

Prox1 regulates the expression of Fgfr3, Lctl and Fgfrl1

This study suggests that, similar to its role in the lymphatic vasculature (Johnson et al., 2008), Prox1 regulates the expression of Fgfr3 in the lens. However, as a single copy of any of the *Fgfr1-3* genes is sufficient to rescue the LF-deficient phenotype in FGFR triple-null mice (Zhao et al., 2008), the downregulation of Fgfr3 alone in *Prox1* cKO lenses does not explain the profound reduction in pERK and pAKT levels observed. Notably though, two other transmembrane FGF-interacting proteins, Lctl and Fgfrl1, might contribute to this phenotype.

Lctl is a transmembrane FGF-binding protein of the Klotho family (Fon Tacer et al., 2010). Signaling through canonical FGFRs requires their association with both FGFs and heparan sulfate (HS) (Schlessinger et al., 2000). Whereas canonical FGFs interact readily with both HS and FGFRs, the FGF19 subfamily has low affinity for HS (Goetz et al., 2007). Thus, FGF19 subfamily members are not sequestered by HS-containing extracellular matrix and can travel further from their origin to act in an endocrine fashion. Their target cells are sensitized to this endocrine signal by expression of Klotho transmembrane receptors, such as Lctl, which bind to FGF19 family members and FGFRs to stabilize the FGF19-HS-FGFR complex, allowing for signal transduction (Goetz et al., 2007; Kurosu et al., 2007). *Lctl* is the only Klotho expressed in the lens (Table 1), and it is the most downregulated gene following Prox1 loss (Table S3), suggesting that it is nearly absent in lenses that do not express Prox1. Lctl would be expected to associate with Fgfr1 and 2 in the lens to facilitate their interaction with Fgf15/19 (Fon Tacer et al., 2010), and thus a loss of Lctl is expected to dramatically decrease the response of Fgfr1 and 2 to endocrine FGFs. Further, we demonstrate that Prox1 binds to the putative *LCTL* promoter in the chicken lens *in vivo*. Therefore, we propose that the onset of Prox1 expression at the lens transition zone might upregulate Lctl levels to sensitize presumptive LFs to FGF19 family members, whereas neighboring epithelial cells, which lack strong nuclear Prox1 expression, would have much lower levels of Lctl and thus not respond to FGF19 protein.

The expression of Fgfrl1, a transmembrane FGFR that lacks an intracellular kinase domain (Steinberg et al., 2010), is downregulated in *Prox1* cKO lenses (Figs 6 and 7). Fgfrl1 was presumed to inhibit FGF signaling by sequestering ligand (Steinberg et al., 2010). However, new evidence suggests that Fgfrl1 facilitates FGF ligand-dependent MAPK activation (Silva et al., 2013). Further, Fgfrl1 also enhanced FGF-stimulated Erk1/2 activation, implicating a role in ligand-dependent signaling (Silva et al., 2013). Intriguingly, Fgfrl1 also increases basal Erk1/2 phosphorylation independently of FGF ligand. Since Fgfrl1 expression is downregulated in *Prox1* cKO lenses, Prox1 expression in the posterior LV is likely to increase Fgfrl1 expression to augment MAPK signal transduction.

Overall, downregulation of these receptors in *Prox1* cKO decreases the FGF signaling capacity of the lens, as Fgfr3 is the most highly expressed of the canonical FGFRs in the lens (Table 1) and interacts with a wide array of paracrine FGF ligands (Robinson, 2006). Fgfrl1 is expressed at even higher levels than Fgfr3 in the lens, and Lctl is required for signaling in response to endocrine Fgf15/19, which is required for lens and retina development in zebrafish and chicken (Kurose et al., 2005; Nakayama et al., 2008). The ChIP experiments suggest that the *Fgfr3*, *Fgfrl1* and *Lctl* promoters are regulated by Prox1; however, further experiments are necessary to definitively show whether the effect of Prox1 on the expression of these FGFRs is direct or indirect.

Prox1 and FGFRs form a novel regulatory loop that regulates the differentiation of lens epithelial cells into LFs

Previous studies have shown that FGF is sufficient to trigger lens epithelial cell differentiation into LFs (Lovicu and McAvoy, 2005). Correspondingly, FGFRs are present at low levels in lens epithelia and the LV, whereas their expression increases dramatically proximal to the onset of LF elongation (de Iongh et al., 1997). If FGFR expression does not reach sufficient levels, LVs are unable to

Development (2016) 143, 318-328 doi:10.1242/dev.127860

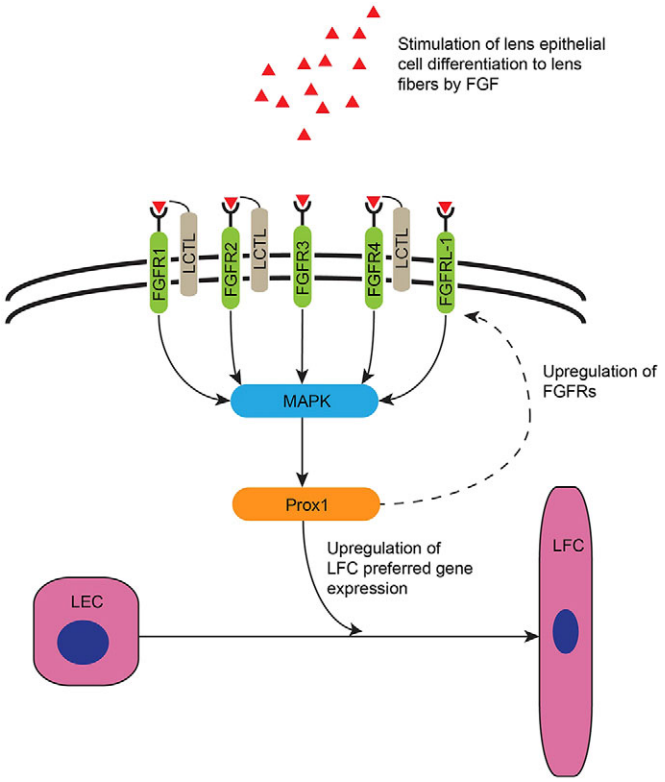

Fig. 9. Model of Prox1 crosstalk with FGFRs. In normal lenses, FGFs interact with the canonical FGFR1-4, or with FGFRL1, to drive intracellular signaling. LCTL facilitates the interaction of FGFR1,2,4 with endocrine FGFs. Activation of FGFRs promotes signaling via the MAPK pathway, upregulating Prox1 expression in response to FGF stimulation. Further, Prox1 upregulates *Fgfr3*, *Fgfrl1* and *Lctl* expression through direct promoter interactions, sensitizing these cells to respond to FGFs, driving LF differentiation. LEC, lens epithelial cell; LFC, lens fiber cell.

respond to FGF, resulting in failure of LF differentiation (Zhao et al., 2008). However, the mechanism by which lens epithelial cells upregulate FGFR expression was previously unclear. Prox1 protein levels are dramatically upregulated in the posterior LV and at the onset of secondary fiber differentiation throughout life (Duncan et al., 2002), a process that is dependent on FGFR signaling in the lens (Li et al., 2014; Zhao et al., 2008). Here, we demonstrate that exogenous FGF is sufficient to stimulate nuclear Prox1 levels in lens explants and that this process requires signaling through the MAPK pathway (see Fig. 8). Thus, we propose that signaling through FGFRs in response to endogenous FGF causes differentiating LFs to increase Prox1 levels. Prox1 may then feedback to transcriptionally upregulate FGFR expression, initiating a positive-feedback loop that rapidly increases FGFR and Prox1 levels. These data implicate Prox1 in this process, but it is possible that Prox1 acts in coordination with as yet unidentified factors (Fig. 9).

In summary, these findings suggest that Prox1 participates in a positive-feedback loop with FGFRs to sensitize differentiating LFs to the surrounding FGF ligand. This process, in turn, is responsible for the regulation of a large proportion of the genes required for LF differentiation.

MATERIALS AND METHODS

Animals

Mice harboring a conditional *Prox1* allele in which exons 3 and 4 (encoding the homeo-prospero domain) are flanked by LoxP sites (Prox1tm2Gco) (Harvey et al., 2005), were obtained from Dr Guillermo Oliver (St Jude Children's Research Hospital, Memphis, TN, USA). These mice were crossed with MLR10Cre mice expressing Cre recombinase throughout the lens beginning at the LV (Zhao et al., 2004), which were obtained from Dr Michael Robinson (Miami University, Oxford, OH, USA) and backcrossed with C57BL/6<Har> for at least four generations. C57BL/6<Har> mice were used as WT controls. E0.5 represents noon of the day the vaginal plug was observed. Mice were genotyped for the *Prox1* flox allele and *MLR10Cre* as described in Table S1. Histology was performed as described previously (Manthey et al., 2014a). No lens defects were observed in mice homozygous or heterozygous for either the *MLR10Cre* transgene or the *Prox1* flox allele alone.

Immunofluorescence

Most immunofluorescence was performed as reported previously (Reed et al., 2001), except that Draq5 (1:2000; Biostatus) was used as the nuclear counterstain and imaging was performed on a Zeiss LSM780 confocal microscope. Specific staining protocols are provided in Table S2. $p57^{Kip2}$ (Santa Cruz, sc8298; 1:100) immunostaining was performed on paraffin sections subjected to antigen retrieval by boiling in 0.01 M sodium citrate buffer pH 6.0, and treatment with 1% Saponin (Sigma-Aldrich). Expression patterns were compared using slides stained simultaneously and scanned using identical imaging settings. Some images were processed to increase brightness or contrast using Photoshop (Adobe Systems); however, all adjustments were applied equally to all images within an experimental/control group.

Immunohistochemistry

Immunohistochemical staining for β-crystallin was performed as described previously (Firtina et al., 2009). Immunohistochemical staining for pErk1/2 (Cell Signaling, cs4377s; 1:50) and pAKT (Cell Signaling, cs9271s; 1:50) was performed on antigen-retrieved paraffin sections using the CSAII Biotin-Free Tyramide Signal Amplification Kit with the CSA II Rabbit Link (Dako, Agilent).

Cell proliferation assays

Cells in S phase were detected using 5-ethynyl-2′-deoxyuridine (EdU) Click-iT cell proliferation assays (Invitrogen). Pregnant mice were injected intraperitoneally with 800 µg EdU. Three hours later, embryos were collected, sectioned, and the Click-it reactions performed as previously described (Mamuya et al., 2014).

TUNEL assay

DNA fragmentation was detected by terminal deoxynucleotidyl transferase dUTP nick end labeling (TUNEL) using the In Situ Cell Death Detection Kit, Fluorescein (Roche). Paraffin sections were subjected to antigen retrieval and TUNEL performed following the manufacturer's directions.

RNA isolation and quantitative real-time PCR (qRT-PCR)

RNA was isolated from lenses collected by the microdissection of E14.5 *Prox1* cKO and WT mice (20 lenses per biological replicate) using the SV Total RNA Kit (Promega). cDNA was synthesized using the SABiosciences RT2 First Strand Kit (Qiagen). qRT-PCR was carried out using QuantiTect SYBR Green (Qiagen) on an ABI7300 Real-Time PCR system (Applied Biosystems) and mRNA levels for each gene were normalized to the 18S ribosomal subunit (Mamuya et al., 2014). Differential expression was determined using the ΔΔCT method (Bookout and Mangelsdorf, 2003) and significance determined by nested ANOVA. The primer sets used for qRT-PCR are listed in Table S1.

RNA-seq

The RNA-seq methods were recently published (Manthey et al., 2014a,b), so only deviations are noted. Embryonic lenses were collected from E13.5 *Prox1* cKO and WT mice by microdissection (30 lenses/sample, three biological replicates/genotype) and total RNA isolated. cDNA libraries were constructed using the Illumina TruSeq RNA Sample Preparation Kit v2, and sequenced using an Illumina HiSeq 2000 (University of Delaware

Development (2016) 143, 318-328 doi:10.1242/dev.127860

Sequencing Center). Reads were processed using the CLC Genomics server, and mapped to the *Mus musculus* GRCm38.77 genome build. Expression level differences between WT and *Prox1* cKO lenses were determined using the EdgeR BioConductor package, using the pairwise qCML method exact test with a Benjamini–Hochberg correction.

The resulting gene list was filtered for statistical significance ($P<0.05$) and expression at greater than 2 RPKM in either *Prox1* cKO or WT lenses (Manthey et al., 2014b). Only genes with a greater than 2.5-fold difference between *Prox1* cKO and WT were considered so as to reduce false positives due to the genetic noise inherent in non-inbred mouse populations (Manthey et al., 2014b).

Bioinformatics analysis of RNA-seq data

The gene lists generated from RNA-seq were analyzed using the DAVID bioinformatics resource (Huang et al., 2009) to identify functionally related gene ontology (GO) categories ascribed to the differentially expressed genes (DEGs). Similar GO terms were grouped/clustered and assigned an enrichment score (DAVID score) to predict biological significance.

Lens-enrichment analysis by the gene prediction tool *iSyTE*

We performed two types of analysis on *Prox1* cKO lens DEGs using the *iSyTE* database. In the first, we investigated the significance of the *Prox1* cKO lens DEGs (642 genes, $P<0.05$) in lens biology by analyzing their normal expression pattern during lens development using *iSyTE* and other publically available lens expression datasets (Lachke et al., 2012). In the second analysis, we determined the proportion of genes downregulated in *Prox1* cKO lens that were among the 100 and 500 most lens-enriched genes calculated by *iSyTE*. *iSyTE* ascribes lens-enrichment scores at various embryonic and postnatal stages in lens development by performing a genome-wide expression comparison (termed '*in silico* subtraction') between microarray datasets for the lens (at stages E10.5, E11.5, E12.5, E16.5, E19.5, P0) with the embryonic whole body (WB) minus eyes reference dataset (Lachke et al., 2012; A. Kakrana and S.A.L., unpublished). The lens-enrichment score for a gene is a measure of its difference in expression [expressed as fold change (FC)] in the lens compared with the whole embryonic body reference at $P<0.05$. Both the above analyses used previously published lens microarray data (GEO datasets GSE32334, GSE47694 and GSE31643) analyzed by an in-house *Python* script (S.A.L. laboratory). The *iSyTE* lens-enrichment scores for DEGs were plotted against their RNA-seq FC. Further, the significance of the differences in lens enrichment for *Prox1* cKO upDEGs and downDEGs was estimated using a χ^2 test followed by a two-tailed *t*-test. The proportion of *Prox1* cKO DEGs in the top 500 and top 100 *iSyTE* lens-enriched genes for different lens stages (E10.5, E11.5, E12.5, E16.5, E19.5, P0) was then estimated.

Phylogenetic foot printing

Gene sequences for *Fgfr1-4*, *Fgfrl1* and *Lctl* were obtained from the human (hg38), mouse (m38.p2) and chicken (4.0, Ensembl release 78) genome assemblies. The −500 to +1 bp regions of these sequences were aligned using CLUSTAL W (Thompson et al., 1994) on the SDSC Biology WorkBench (v3.2) (Subramaniam, 1998). These regions were analyzed for the known Prox1 binding sites: 1, CA(not A)(N)(N)(C or G)(C or T); and 2, (A or C) AAG(N)(not A) (Chen et al., 2008) using PATTERNMATCH (Subramaniam, 1998) and overlaid upon the multiple sequence alignments to assess evolutionary conservation.

Chromatin immunoprecipitation

Lenses were collected from E14.5 chicken embryos, and 180 mg pooled samples were fixed for 5 min in 1% formaldehyde, flash frozen and pulverized using a Covaris CryoPREP. Nuclei were extracted and processed using the truChIP Chromatin Shearing Kit (Covaris) and chromatin sheared using a Covaris S2 adaptive focused acoustic disrupter. ChIP was carried out using 100 µg chromatin per sample, pulling down with 1 µl anti-Prox1 (Chen et al., 2008). Crosslinks were reversed and samples were analyzed by quantitative PCR. All primers are listed in Table S1. These data were normalized to 1% input (Haring et al., 2007) and were analyzed by two-way ANOVA using planned comparisons against the +5 kb region of each gene.

Rat lens explant culture

Rat lens epithelial explants were prepared as described previously (Wang et al., 2010). Explants were cultured for 5 days in the absence (control) or presence of human recombinant FGF2 (100 ng/ml; Peprotech, 1001B), and in the presence or absence of the following inhibitors: FGFR antagonist SU5402 (Sigma-Aldrich, SML0443); MEK inhibitor UO126 (Cell Signaling, 9903S); PI3K/AKT inhibitor LY294002 (Cell Signaling, 9901S). For immunofluorescence, explants were immunostained for Prox1, as above, with Hoechst (nuclear stain), and for β-catenin (Wang et al., 2010).

For western blotting, cell lysates were prepared as previously described (Zhao et al., 2015), with the addition of a phosphatase inhibitor cocktail (Roche, 04906845001). Membranes were blocked and then incubated in primary antibody, either Prox1 [1:1000 (Chen et al., 2008)] or Gapdh (1:5000; Sigma-Aldrich, G8795), overnight at 4°C, and rinsed. The membrane was then incubated with either anti-rabbit (Cell Signaling, 7074; 1:5000) or anti-mouse (Zymed, 62-6520; 1:10,000) HRP-conjugated secondary antibodies. Enhanced chemiluminescence (Millipore, WBKLS0500) was used to detect protein bands. Resultant bands from three independent experiments were captured using the ChemiDoc MP imaging system (Bio-Rad) and band intensities quantified using Image Lab software (version 4.0, Bio-Rad). Statistical significance was assessed using a non-parametric one-way ANOVA test followed by a Šídák multiple comparison post-test, with data reported as mean±s.e.m.

Acknowledgements

We thank Brewster Kingman of the University of Delaware Sequencing and Genotyping Center and Dr Shawn Polson of the University of Delaware Center for Bioinformatics and Computational Biology, for technical support of the RNA-seq experiment. We thank the staff of the University of Delaware Bioimaging facility for their excellent support of the microscopes used in this work. These core facilities are supported by grants from the NIH National Center for Research Resources [05 P20 RR016472-12], the NIH National Institute of General Medical Sciences [8 P20 GM103446-12], and National Science Foundation EPSCoR [EPS-081425].

Competing interests

The authors declare no competing or financial interests.

Author contributions

D.S.A. is the lead author and contributed to the concept and design, performed experiments and analyzed data. D.A. designed and implemented the DEG systems analysis and edited this work. T.S. performed the rat lens explant experiments. T.B.R. helped develop and perform immunohistochemistry. S.A.L. contributed to the concept and design, provided financial support, and helped design the systems analysis of DEGs, and edited the manuscript. F.J.L. contributed to the concept of this work, provided financial support, and edited the manuscript. M.K.D. is the senior author, developed the concept, revised the manuscript, and provided financial support. D.S.A., D.A., F.J.L., S.A.L. and M.K.D. wrote the manuscript and all authors read and approved the final manuscript.

Funding

This work was supported by grants from the National Institutes of Health (NIH)/National Eye Institute to M.K.D. [R01 EY012221], S.A.L. [R01 EY021505] and F.J.L. [R01 EY03177]; and grants from the Delaware Institutional Networks for Biomedical Research Excellence [GM103446]. The confocal microscope used in this study was acquired via an NIH major instrumentation grant [1S10 RR027273-01]. Deposited in PMC for release after 12 months.

Supplementary information

Supplementary information available online at
http://dev.biologists.org/lookup/suppl/doi:10.1242/dev.127860/-/DC1

References

Bassnett, S., Wilmarth, P. A. and David, L. L. (2009). The membrane proteome of the mouse lens fiber cell. *Mol. Vis.* **15**, 2448-2463.

Bhat, S. P. (2001). The ocular lens epithelium. *Biosci. Rep.* **21**, 537-563.

Bookout, A. L. and Mangelsdorf, D. J. (2003). Quantitative real-time PCR protocol for analysis of nuclear receptor signaling pathways. *Nucl. Recept. Signal.* **1**, e012.

Chen, X., Taube, J. R., Simirskii, V. I., Patel, T. P. and Duncan, M. K. (2008). Dual roles for Prox1 in the regulation of the chicken betaB1-crystallin promoter. *Invest. Ophthalmol. Vis. Sci.* **49**, 1542-1552.

Cross, M. and Dexter, T. M. (1991). Growth factors in development, transformation, and tumorigenesis. *Cell* **64**, 271-280.
Cui, W., Tomarev, S. I., Piatigorsky, J., Chepelinsky, A. B. and Duncan, M. K. (2004). Mafs, Prox1, and Pax6 can regulate chicken betaB1-crystallin gene expression. *J. Biol. Chem.* **279**, 11088-11095.
Dash, S., Dang, C. A., Beebe, D. C. and Lachke, S. A. (2015). Deficiency of the RNA binding protein caprin2 causes lens defects and features of peters anomaly. *Dev. Dyn.* **244**, 1313-1327.
de Iongh, R. U. and Duncan, M. K. (2015). Lens epithelium and posterior capsular opacification | Springer. In *Lens Epithelium and Posterior Capsular Opacification* (ed. S. Saika, L. Werner and F. J. Lovicu), pp. 81-104. Tokyo, Japan: Springer.
de Iongh, R. U., Lovicu, F. J., Chamberlain, C. G. and McAvoy, J. W. (1997). Differential expression of fibroblast growth factor receptors during rat lens morphogenesis and growth. *Invest. Ophthalmol. Vis. Sci.* **38**, 1688-1699.
Duncan, M. K., Cui, W., Oh, D.-J. and Tomarev, S. I. (2002). Prox1 is differentially localized during lens development. *Mech. Dev.* **112**, 195-198.
Duncan, M., Cvekl, A., Kantorow, M. and Piatigorsky, J. (2004). Lens crystallins. In *Development of the Ocular Lens* (ed. F. Lovicu and M. Robinson), pp. 119-150. Cambridge, UK: Cambridge University Press.
Firtina, Z., Danysh, B. P., Bai, X., Gould, D. B., Kobayashi, T. and Duncan, M. K. (2009). Abnormal expression of Collagen IV in lens activates unfolded protein response resulting in cataract. *J. Biol. Chem.* **284**, 35872-35884.
Fon Tacer, K., Bookout, A. L., Ding, X., Kurosu, H., John, G. B., Wang, L., Goetz, R., Mohammadi, M., Kuro-o, M., Mangelsdorf, D. J. et al. (2010). Research resource: Comprehensive expression atlas of the fibroblast growth factor system in adult mouse. *Mol. Endocrinol.* **24**, 2050-2064.
Fromm, L., Shawlot, W., Gunning, K., Butel, J. S. and Overbeek, P. A. (1994). The retinoblastoma protein-binding region of simian virus 40 large T antigen alters cell cycle regulation in lenses of transgenic mice. *Mol. Cell. Biol.* **14**, 6743-6754.
Goetz, R., Beenken, A., Ibrahimi, O. A., Kalinina, J., Olsen, S. K., Eliseenkova, A. V., Xu, C., Neubert, T. A., Zhang, F., Linhardt, R. J. et al. (2007). Molecular insights into the klotho-dependent, endocrine mode of action of fibroblast growth factor 19 subfamily members. *Mol. Cell. Biol.* **27**, 3417-3428.
Haring, M., Offermann, S., Danker, T., Horst, I., Peterhansel, C. and Stam, M. (2007). Chromatin immunoprecipitation: optimization, quantitative analysis and data normalization. *Plant Methods* **3**, 11.
Harvey, N. L., Srinivasan, R. S., Dillard, M. E., Johnson, N. C., Witte, M. H., Boyd, K., Sleeman, M. W. and Oliver, G. (2005). Lymphatic vascular defects promoted by Prox1 haploinsufficiency cause adult-onset obesity. *Nat. Genet.* **37**, 1072-1081.
Hawse, J. R., DeAmicis-Tress, C., Cowell, T. L. and Kantorow, M. (2005). Identification of global gene expression differences between human lens epithelial and cortical fiber cells reveals specific genes and their associated pathways important for specialized lens cell functions. *Mol. Vis.* **11**, 274-283.
Huang, D. W., Sherman, B. T. and Lempicki, R. A. (2009). Systematic and integrative analysis of large gene lists using DAVID bioinformatics resources. *Nat. Protoc.* **4**, 44-57.
Johnson, N. C., Dillard, M. E., Baluk, P., McDonald, D. M., Harvey, N. L., Frase, S. L. and Oliver, G. (2008). Lymphatic endothelial cell identity is reversible and its maintenance requires Prox1 activity. *Genes Dev.* **22**, 3282-3291.
Kim, J. I., Li, T., Ho, I.-C., Grusby, M. J. and Glimcher, L. H. (1999). Requirement for the c-Maf transcription factor in crystallin gene regulation and lens development. *Proc. Natl. Acad. Sci. USA* **96**, 3781-3785.
Kurose, H., Okamoto, M., Shimizu, M., Bito, T., Marcelle, C., Noji, S. and Ohuchi, H. (2005). FGF19-FGFR4 signaling elaborates lens induction with the FGF8-L-Maf cascade in the chick embryo. *Dev. Growth Differ.* **47**, 213-223.
Kurosu, H., Choi, M., Ogawa, Y., Dickson, A. S., Goetz, R., Eliseenkova, A. V., Mohammadi, M., Rosenblatt, K. P., Kliewer, S. A. and Kuro-o, M. (2007). Tissue-specific expression of betaKlotho and fibroblast growth factor (FGF) receptor isoforms determines metabolic activity of FGF19 and FGF21. *J. Biol. Chem.* **282**, 26687-26695.
Lachke, S. A., Alkuraya, F. S., Kneeland, S. C., Ohn, T., Aboukhalil, A., Howell, G. R., Saadi, I., Cavallesco, R., Yue, Y., Tsai, A. C.-H. et al. (2011). Mutations in the RNA granule component TDRD7 cause cataract and glaucoma. *Science* **331**, 1571-1576.
Lachke, S. A., Ho, J. W. K., Kryukov, G. V., O'Connell, D. J., Aboukhalil, A., Bulyk, M. L., Park, P. J. and Maas, R. L. (2012). iSyTE: integrated systems tool for eye gene discovery. *Invest. Ophthalmol. Vis. Sci.* **53**, 1617-1627.
Lengler, J., Krausz, E., Tomarev, S., Prescott, A., Quinlan, R. A. and Graw, J. (2001). Antagonistic action of Six3 and Prox1 at the gamma-crystallin promoter. *Nucleic Acids Res.* **29**, 515-526.
Li, H., Tao, C., Cai, Z., Hertzler-Schaefer, K., Collins, T. N., Wang, F., Feng, G.-S., Gotoh, N. and Zhang, X. (2014). Frs2α and Shp2 signal independently of Gab to mediate FGF signaling in lens development. *J. Cell Sci.* **127**, 571-582.
Lovicu, F. J. and McAvoy, J. W. (2005). Growth factor regulation of lens development. *Dev. Biol.* **280**, 1-14.
Lovicu, F. J., McAvoy, J. W. and de Iongh, R. U. (2011). Understanding the role of growth factors in embryonic development: insights from the lens. *Philos. Trans. R. Soc. Lond. B Biol. Sci.* **366**, 1204-1218.
Mamuya, F. A., Wang, Y., Roop, V. H., Scheiblin, D. A., Zajac, J. C. and Duncan, M. K. (2014). The roles of alphaV integrins in lens EMT and posterior capsular opacification. *J. Cell. Mol. Med.* **18**, 656-670.
Manthey, A. L., Lachke, S. A., FitzGerald, P. G., Mason, R. W., Scheiblin, D. A., McDonald, J. H. and Duncan, M. K. (2014a). Loss of Sip1 leads to migration defects and retention of ectodermal markers during lens development. *Mech. Dev.* **131**, 86-110.
Manthey, A. L., Terrell, A. M., Lachke, S. A., Polson, S. W. and Duncan, M. K. (2014b). Development of novel filtering criteria to analyze RNA-sequencing data obtained from the murine ocular lens during embryogenesis. *Genom. Data* **2**, 369-374.
McAvoy, J. W. and Chamberlain, C. G. (1989). Fibroblast growth factor (FGF) induces different responses in lens epithelial cells depending on its concentration. *Development* **107**, 221-228.
Nakayama, Y., Miyake, A., Nakagawa, Y., Mido, T., Yoshikawa, M., Konishi, M. and Itoh, N. (2008). Fgf19 is required for zebrafish lens and retina development. *Dev. Biol.* **313**, 752-766.
Nishiguchi, S., Wood, H., Kondoh, H., Lovell-Badge, R. and Episkopou, V. (1998). Sox1 directly regulates the gamma-crystallin genes and is essential for lens development in mice. *Genes Dev.* **12**, 776-781.
Pan, H. and Griep, A. E. (1994). Altered cell cycle regulation in the lens of HPV-16 E6 or E7 transgenic mice: implications for tumor suppressor gene function in development. *Genes Dev.* **8**, 1285-1299.
Piatigorsky, J. (1975). Lens cell elongation in vitro and microtubules. *Ann. N. Y. Acad. Sci.* **253**, 333-347.
Reed, N. A., Oh, D. J., Czymmek, K. J. and Duncan, M. K. (2001). An immunohistochemical method for the detection of proteins in the vertebrate lens. *J. Immunol. Methods* **253**, 243-252.
Robinson, M. L. (2006). An essential role for FGF receptor signaling in lens development. *Semin. Cell Dev. Biol.* **17**, 726-740.
Scata, K. A., Bernard, D. W., Fox, J. and Swain, J. L. (1999). FGF receptor availability regulates skeletal myogenesis. *Exp. Cell Res.* **250**, 10-21.
Schlessinger, J., Plotnikov, A. N., Ibrahimi, O. A., Eliseenkova, A. V., Yeh, B. K., Yayon, A., Linhardt, R. J. and Mohammadi, M. (2000). Crystal structure of a ternary FGF-FGFR-heparin complex reveals a dual role for heparin in FGFR binding and dimerization. *Mol. Cell* **6**, 743-750.
Shaham, O., Smith, A. N., Robinson, M. L., Taketo, M. M., Lang, R. A. and Ashery-Padan, R. (2009). Pax6 is essential for lens fiber cell differentiation. *Development* **136**, 2567-2578.
Shin, J. W., Min, M., Larrieu-Lahargue, F., Canron, X., Kunstfeld, R., Nguyen, L., Henderson, J. E., Bikfalvi, A., Detmar, M. and Hong, Y.-K. (2006). Prox1 promotes lineage-specific expression of fibroblast growth factor (FGF) receptor-3 in lymphatic endothelium: a role for FGF signaling in lymphangiogenesis. *Mol. Biol. Cell* **17**, 576-584.
Silva, P. N., Altamentova, S. M., Kilkenny, D. M. and Rocheleau, J. V. (2013). Fibroblast growth factor receptor like-1 (FGFRL1) interacts with SHP-1 phosphatase at insulin secretory granules and induces beta-cell ERK1/2 protein activation. *J. Biol. Chem.* **288**, 17859-17870.
Steinberg, F., Zhuang, L., Beyeler, M., Kälin, R. E., Mullis, P. E., Brändli, A. W. and Trueb, B. (2010). The FGFRL1 receptor is shed from cell membranes, binds fibroblast growth factors (FGFs), and antagonizes FGF signaling in Xenopus embryos. *J. Biol. Chem.* **285**, 2193-2202.
Streit, A. (2004). Early development of the cranial sensory nervous system: from a common field to individual placodes. *Dev. Biol.* **276**, 1-15.
Subramaniam, S. (1998). The Biology Workbench—a seamless database and analysis environment for the biologist. *Proteins* **32**, 1-2.
Thompson, J. D., Higgins, D. G. and Gibson, T. J. (1994). CLUSTAL W: improving the sensitivity of progressive multiple sequence alignment through sequence weighting, position-specific gap penalties and weight matrix choice. *Nucleic Acids Res.* **22**, 4673-4680.
Tomarev, S. I., Sundin, O., Banerjee-Basu, S., Duncan, M. K., Yang, J.-M. and Piatigorsky, J. (1996). Chicken homeobox gene Prox1 related to Drosophila prospero is expressed in the developing lens and retina. *Dev. Dyn.* **206**, 354-367.
Wang, Q., Stump, R., McAvoy, J. W. and Lovicu, F. J. (2009). MAPK/ERK1/2 and PI3-kinase signalling pathways are required for vitreous-induced lens fibre cell differentiation. *Exp. Eye Res.* **88**, 293-306.
Wang, Q., McAvoy, J. W. and Lovicu, F. J. (2010). Growth factor signaling in vitreous humor–induced lens fiber differentiation. *Invest. Ophthalmol. Vis. Sci.* **51**, 3599-3610.
Weber, G. F. and Menko, A. S. (2006a). Actin filament organization regulates the induction of lens cell differentiation and survival. *Dev. Biol.* **295**, 714-729. United States.
Weber, G. F. and Menko, A. S. (2006b). Phosphatidylinositol 3-kinase is necessary for lens fiber cell differentiation and survival. *Invest. Ophthalmol. Vis. Sci.* **47**, 4490-4499.
Wigle, J. T. and Oliver, G. (1999). Prox1 function is required for the development of the murine lymphatic system. *Cell* **98**, 769-778.
Wigle, J. T., Chowdhury, K., Gruss, P. and Oliver, G. (1999). Prox1function is crucial for mouse lens-fibre elongation. *Nat. Genet.* **21**, 318-322.

Development (2016) 143, 318-328 doi:10.1242/dev.127860

Zhang, P., Wong, C., DePinho, R. A., Harper, J. W. and Elledge, S. J. (1998). Cooperation between the Cdk inhibitors p27(KIP1) and p57(KIP2) in the control of tissue growth and development. *Genes Dev.* **12**, 3162-3167.

Zhao, H., Yang, Y., Rizo, C. M., Overbeek, P. A. and Robinson, M. L. (2004). Insertion of a Pax6 consensus binding site into the alphaA-crystallin promoter acts as a lens epithelial cell enhancer in transgenic mice. *Invest. Ophthalmol. Vis. Sci.* **45**, 1930-1939.

Zhao, H., Yang, T., Madakashira, B. P., Thiels, C. A., Bechtle, C. A., Garcia, C. M., Zhang, H., Yu, K., Ornitz, D. M., Beebe, D. C. et al. (2008). Fibroblast growth factor receptor signaling is essential for lens fiber cell differentiation. *Dev. Biol.* **318**, 276-288.

Zhao, G., Wojciechowski, M. C., Jee, S., Boros, J., McAvoy, J. W. and Lovicu, F. J. (2015). Negative regulation of TGFbeta-induced lens epithelial to mesenchymal transition (EMT) by RTK antagonists. *Exp. Eye Res.* **132**, 9-16.

Supplementary Table 1: primers

gene	target	species	forward	reverse
Prox1	DNA	mouse	CTC TGT GGA AAG GAC TCC GAA TC	ACA CTA AAC AAG CAA ATG GAA ATG C
MLR10Cre	DNA	mouse	CCT GTT TTG CAC GTT CAC CG	ATG CTT CTG TCC GTT TGC CG
Cdkn1b	mRNA	mouse	GCC AGA CGT AAA CAG CTC CGA ATT A	AGG CAG ATG GTT TAA GAG TGC CT
Cdkn1C	mRNA	mouse	CAA GCG AAC AGG CAG GCA AGC	TCG AAG GCT GGC TGA TTG GTG
Maf	mRNA	mouse	GTG GTG GTG ATG GCT CTT TT	GTT ACG GGG GAA TTC AGG TT
Cryaa	mRNA	mouse	GAG ATT CAC GGC AAA CAC AA	ACA TTG GAA GGC AGA CGG TA
Cryab	mRNA	mouse	ACT CAA AGT CAA GGT TCT GGG	GGG ATG AAG TGA TGG TGA GAG
Cryba1	mRNA	mouse	TGG AGT GTG GCG CCT GGA TT	CAT TGC TCC CGC TCC AGG CAT
Cryba3/a1	mRNA	mouse	CCT GGA GCG GGA GCA ATG CC	TCA CAG ATT TCC CAC TGG CGT CC
Crybb2	mRNA	mouse	GTG CAG AGC GGC ACG TGG GT	TGT CAC GGA TGC GAC GCA CA
Crygc	mRNA	mouse	CAT CCC CCA TGC AGG TTC	AGC CCG CCT TAG CAT CTA CA
Fgfr1	mRNA	mouse	AGC CCC TCT GGC AGC GAT ACC	AGG GAG CTA CAG GCC TAC GGT T
Fgfr2	mRNA	mouse	GGG GGC GCT TCA TCT GCC TG	CGG TGC TCC TTC TGG TTC TAA AGT G
Fgfr3	mRNA	mouse	CAG TGT GCG TGT AAC AGA TGC TCC A	TCG CTC CGG GCG AGT CCA AT
Lctl	mRNA	mouse	GCA CTG GCC TAT ATG TGG CT	TAC TAG GCC GTG CTG TTT GC
Mafb	mRNA	mouse	GCC TCT TAG ACT TGG GCA GA	CCT TCC AGC TTG GAG AA AG
Mip	mRNA	mouse	CGT GCT CTG CAT CTT TGC TA	ACC CTC CCC ACA GTC TCT TT
Pax6	mRNA	mouse	GCA CAT GCA AAC ACA CAT GA	ACT TGG ACG GGA ACT GAC AC
Prox1	mRNA	mouse	AGT AAG ACA TCA CCG CGT GCG C	GCT GGG CAC AGC TCA AGA ATC CC
Sox1	mRNA	mouse	GGC CAA GCG GCT GCG CGC GCT	GGC CAG CTG CGC CTC CTG CAT
Sox2	mRNA	mouse	GGC AGC TAC AGC ATG ATG CAG GAG C	CTG GTC ATG GAG TTG TAC TGC AGG
Crybb1	mRNA	mouse	CAG GGC CTG ATG GCA AGG GAA	CCT GCT CGA AGA CGA TCA GCC
Cdh1	mRNA	mouse	GCACTCTTCTCCTGGTCCTG	TATGAGGCTGTGGGTTCCCTC
Fgfrl1	mRNA	mouse	TCT TCA GGC TTC AGG TTC TTC AAG C	AGG AGG ACC CAG CCA GC
18S rDNA	RNA	mouse	QUIAGEN PPM57735E-200	
-0.15 Kb Crybb1	DNA	chicken	TCT GTT GTG CCG CTG GAT A	CCA GTC ATC ACA TCC TGC AA
-.05 Kb Spam1	DNA	chicken	AGC TGC ACT CCA GTC CTT TC	GTA GCC TCT GGC ATG GTG TT
-2 Kb Lctl	DNA	chicken	AGG AAG ATG TCT CAC CCC TGA	TCC CTC CTG CAA TAG GTG GTA
-0.4 Kb Lctl	DNA	chicken	CCC AGT GGG GGA GCA ATA AA	TGT ATC GAA GTG ACA TCA GCG
-0.05 Kb Lctl	DNA	chicken	ATT CAC AGG CTG GAA ACT CC	TGT ACA ATG CGG GAG AAG TGA
+5 Kb Lctl	DNA	chicken	AGC CTG GCT TGC ATG TGT AT	GGA GTG TTC AGA AGT GTG GGA
-2 Kb Fgfr3	DNA	chicken	GAG AGG CTC AGA CAC CGA AC	AGT CTC CTG CTG AGT GAC CA
-0.14 Kb Fgfr3	DNA	chicken	TCC CAT CCC CGT ATT CAG GA	ATG TGT TCG GTG TCT GAG CC
+5 Kb Fgfr3	DNA	chicken	ACT GAC TCC ATG CTC TCC CT	GCA GGC AGC AAA ACT TCC AA
-2 Kb Fgfrl1	DNA	chicken	TCT GGA TGC CCA AAG ATG GAG	TGC CTC CTG TAG ACT TTC CCA
-0.038 Kb Fgfrl1	DNA	chicken	AGC TCA TCT CAG GAA ACG GC	CAT AGG CTG CGT GTC CAT CT
-0.15 Kb Fgfrl1	DNA	chicken	TGC CCG TGG CGG TTG	AGC TCC AAA CTT CGC TCC AA
+5 Kb Fgfrl1	DNA	chicken	TTC TCT CTG CAC CAC TTG GC	TAG TCC CAA CAA CAC GTT CCC
Prox1	mRNA	chicken	AGA TGG AGA AGT ATG CGC GG	CTG GAA CCT CAA AGT CAT TCG C
Fgfr1	mRNA	chicken	GGG GTA CAA GGT CCG CTA TG	GTG TGG TTG ATG CTC CCG TA
Fgfr2	mRNA	chicken	TCT GCC AGC TCC TGA AAA GG	TTC TTC ATG CGG CAC AGG AT
Fgfr3	mRNA	chicken	GGA AAC CCA ACT CCC ACC AT	GCT GGT GTC GCA ACT TGA TG
Fgfrl1	mRNA	chicken	CAG TCC TGC CAG ATC CCA AG	GCA AAG CCA CAG GAG GAT TG
Lctl	mRNA	chicken	TCA CAC TCT GCA TAC TCA CCA G	ACA GCT GGC TTA CTG TAT TGT
18s	mRNA	chicken	TGT GCC GCT AGA GGT GAA ATT	TGG CAA ATG CTT TCG CTT T

Development • Supplementary information

Supplementary Table 2: immunofluorescence and immunohistochemistry procedures

Gene Symbol	Antibody	Sample Prep	Fixation	Blocking	Primary	secondary	final wash
Prox1	from Duncan MK et al. 2002	Frozen tissue was sectioned (16uM) and stored at -80C	immersion in 1:1 acetone/methanol at -20C for 15 minutes, then slides were air dried	Slides were immersed in 1% Bovine Serum Albumin (BSA) in Phosphate buffered saline (PBS) for 1 hour at room temperature (RT).	Primary antibody was diluted 1:500 in blocking buffer, and applied to tissue for 1 hour at RT in a humid slide chamber. Slides were then washed 3 times for 5 minutes in PBS.	Secondary Alexafluor 568 conjugated anti-rabbit antibody was diluted 1:200 in blocking buffer with 1:2000 Draq5, and applied to tissue for 1 hour at RT in a humid slide chamber.	Slides were washed 3 times for ten minutes with PBS then covered with mounting media, coverslipped and sealed, slides were stored at -20C until imaged.
cMaf	Santa Cruz: sc-7866	Frozen tissue was sectioned (16uM) and stored at -80C	immersion in 1:1 acetone/methanol at -20C for 15 minutes, then slides were air dried	Slides were immersed in 1% Bovine Serum Albumin (BSA) in Phosphate buffered saline (PBS) for 1 hour at room temperature (RT).	Primary antibody was diluted 1:100 in blocking buffer, and applied to tissue for 1 hour at RT in a humid slide chamber. Slides were then washed 3 times for 5 minutes in PBS.	Secondary Alexafluor 568 conjugated anti-rabbit antibody was diluted 1:200 in blocking buffer with 1:2000 Draq5, and applied to tissue for 1 hour at RT in a humid slide chamber.	Slides were washed 3 times for ten minutes with PBS then covered with mounting media, coverslipped and sealed, slides were stored at -20C until imaged.
Pax6	Santa Cruz: sc-53106	Frozen tissue was sectioned (16uM) and stored at -80C	immersion in 4% paraformaldehyde (pfa) in PBS for 20 min @ RT, then slides were washed in tris buffered saline (TBS) for 5 minutes.	Samples were covered with 5% normal goat serum in TBS supplemented with .3% Triton x100	Primary antibody was diluted 1:200 in blocking buffer, and applied to tissue overnight in a humid slide chamber at 4C. Slides were then washed 3 times for 10 minutes in TBS.	Secondary Alexafluor 568 conjugated anti-rabbit antibody was diluted 1:200 in blocking buffer with 1:2000 Draq5, and applied to tissue for 1 hour at RT in a humid slide chamber.	Slides were washed 3 times for ten minutes with TBS then covered with mounting media, coverslipped and sealed, slides were stored at -20C until imaged.
ECad	Cell Signaling : 4065	Frozen tissue was sectioned (16uM) and stored at -80C	immersion in 4% paraformaldehyde (pfa) in PBS for 20 min @ RT, then slides were washed in tris buffered saline (TBS) for 5 minutes.	Samples were covered with 5% normal goat serum in TBS supplemented with .3% Triton x100	Primary antibody was diluted 1:100 in blocking buffer, and applied to tissue overnight in a humid slide chamber at 4C. Slides were then washed 3 times for 10 minutes in TBS.	Secondary Alexafluor 568 conjugated anti-rabbit antibody was diluted 1:200 in blocking buffer with 1:2000 Draq5, and applied to tissue for 1 hour at RT in a humid slide chamber.	Slides were washed 3 times for ten minutes with TBS then covered with mounting media, coverslipped and sealed, slides were stored at -20C until imaged.
Cdnk1b ($p27^{Kip1}$)	Santa Cruz: sc-528	Frozen tissue was sectioned (16uM) and stored at -80C	immersion in 4% paraformaldehyde (pfa) in PBS for 20 min @ RT, then slides were washed in tris buffered saline (TBS) for 5 minutes.	Samples were covered with 5% normal goat serum in TBS supplemented with .3% Triton x100	Primary antibody was diluted 1:100 in blocking buffer, and applied to tissue overnight in a humid slide chamber at 4C. Slides were then washed 3 times for 10 minutes in TBS.	Secondary Alexafluor 568 conjugated anti-rabbit antibody was diluted 1:200 in blocking buffer with 1:2000 Draq5, and applied to tissue for 1 hour at RT in a humid slide chamber.	Slides were washed 3 times for ten minutes with TBS then covered with mounting media, coverslipped and sealed, slides were stored at -20C until imaged.
Mip (Aqp0)	Millipore : AB3071	Frozen tissue was sectioned (16uM) and stored at -80C	immersion in 1:1 acetone/methanol at -20C for 15 minutes, then slides were air dried	Slides were immersed in 1% Bovine Serum Albumin (BSA) in Phosphate buffered saline (PBS) for 1 hour at room temperature (RT).	Primary antibody was diluted 1:100 in blocking buffer, and applied to tissue for 1 hour at RT in a humid slide chamber. Slides were then washed 3 times for 5 minutes in PBS.	Secondary Alexafluor 568 conjugated anti-rabbit antibody was diluted 1:200 in blocking buffer with 1:2000 Draq5, and applied to tissue for 1 hour at RT in a humid slide chamber.	Slides were washed 3 times for ten minutes with PBS then covered with mounting media, coverslipped and sealed, slides were stored at -20C until imaged.

Cdkn 1c (p57 ^{Kip2})	Santa Cruz: sc-8298	Paraffin embedded tissue was sectioned (6uM) and stored at RT	sections were dewaxed by two five minute immersions in xylenes, then 2 minute immersions in decreasing concentrations of ethanol in water (100%, 95%, 70%, 50%) followed by a brief rinse in running distilled water.	Antigen retrieval: slides were double boiled in 0.1M Sodium citrate pH6.0 for 30 minutes, and allowed to cool for 10 minutes. Slides were rinsed in dH2O for 2 minutes and washed in PBS for 5 minutes. Slides were immersed in 1% Saponin in PBS for 5 minutes, followed by 3 5 minute immersions in PBS with 0.1% Tween 20 (PBS-T). Slides were then blocked in 10% NGS in PBST for 30 minutes at RT.	Primary antibody was diluted 1:100 in blocking buffer, and applied to tissue overnight in a humid slide chamber at 4C. Slides were then washed 3 times for 10 minutes in PBS.	Secondary Alexafluor 568 conjugated anti-rabbit antibody was diluted 1:200 in blocking buffer with 1:2000 Draq5, and applied to tissue for 2 hours at RT in a humid slide chamber.	Slides were washed 3 times for ten minutes with PBS then covered with mounting media, coverslipped and sealed, slides were stored at -20C until imaged.
Cryg (gamma-crystallin)	Santa Cruz: sc-22415	Frozen tissue was sectioned (16uM) and stored at -80C	immersion in 4% paraformaldehyde (pfa) in PBS for 20 min @ RT, then slides were washed in tris buffered saline (PBS) for 5 minutes.	Samples were covered with 5% normal chicken serum in PBS supplimented with .3% Triton x100	Primary antibody was diluted 1:100 in blocking buffer, and applied to tissue for 4 hours in a humid slide chamber at RT. Slides were then washed 3 times for 10 minutes in PBS.	Secondary Alexafluor 568 conjugated anti-rabbit antibody was diluted 1:200 in blocking buffer with 1:2000 Draq5, and applied to tissue for 2 hours at RT in a humid slide chamber.	Slides were washed 3 times for ten minutes with PBS then covered with mounting media, coverslipped and sealed, slides were stored at -20C until imaged.
Cryb (beta-crystallin	gift from Samuel Zigler, Johns Hopkins Universit y , MD)	Paraffin embedded tissue was sectioned (6uM) and stored at RT	paraffin sections were de-waxed by two immersions in Citrus Clearing Solvent for 10 minutes. Samples were rehydrated by immersion in decreeing concentrations of ethanol in water (100% 3x 3min, 95% 3x 2min, 70% 2 min.	Samples were processed using the Dako Envision horseraddish peroxidase (HRP) kit. Endogenous peroxides were eliminated covering samples with peroxidase blocking solution.	Primary antibody was diluted 1:600 in PBST and incubated in a humid slide chamber for 30 minutes at RT.	Slides were treated with anti rabbit conjugated HRP for 30 min and washed in PBS 3 times for five minutes. Slides were treated with 3,3'-diaminobenzidine (DAB) chromogen in pairs of controls and experimental slides until the tissue was visibly stained.	Slides were counterstained with Hematoxylin, and dehydrated and sealed according to our H&E protocol.
p-ERK (phosph orylated ERK	Cell Signaling : 4377s	Paraffin embedded tissue was sectioned (6uM) and stored at RT	paraffin sections were de-waxed by two immersions in Citrus Clearing Solvent for 10 minutes. Samples were rehydrated by immersion in decreeing concentrations of ethanol in water (100% 3x 3min, 95% 3x 2min, 70% 2 min.	Antigen retrieval: slides were double boiled in 0.1M Sodium citrate pH6.0 for 30 minutes, and allowed to cool for 10 minutes. Slides were rinsed in dH2O for 2 minutes and washed in PBS for 5 minutes. Slides were immersed in 1% Saponin in PBS for 5 minutes, followed by 3 5 minute immersions in PBS with 0.1% Tween 20 (PBS-T). Slides were then blocked in 10% NGS in PBST for 30 minutes at RT.	Slides were processed using the standard procedure outlined in the CSAII Biotin-Free Tyramide Signal Amplification kit with the CSAII rabbit link addition from DAKO. Primary antibody was diluted 1:50.		Slides were counterstained with Hematoxylin, and dehydrated and sealed according to our H&E protocol.

p-AKT (Phosphorylated AKT)	Cell Signaling : 9271s	Paraffin embedded tissue was sectioned (6uM) and stored at RT	paraffin sections were de-waxed by two immersions in Citrus Clearing Solvent for 10 minutes. Sampes were rehydrated by immersion in decreseing concentrations of ethanol in water (100% 3x 3min, 95% 3x 2min, 70% 2 min.	Antigen retreival: slides were double boiled in 0.1M Sodium citrate pH6.0 for 30 minutes, and allowed to cool for 10 minutes. Slides were rinsed in dH2O for 2 minutesand washed in PBS for 5 minutes. Slides were immersed in 1% Saponin in PBS for 5 minutes, followed by 3 5 minute immersions in PBS with 0.1% Tween 20 (PBS-T). Slides were then blocked in 10% NGS in PBST for 30 minutes at RT.	Slides were processed using the standard procedure outlined in the CSAII Biotin-Free Tyramide Signal Amplification kit with the CSAII rabbit link addition from DAKO. Primary antibody was diluted 1:50.	Slides were counterstained with Hematoxylin, and dehydrated and sealed according to our H&E protocol.

Supplementary Table 3: genes down-regulated following Prox1 loss

feature ID	fold change	FDR Pvalue	ensembl gene id	Prox1 rpkm mean	C57 rpkm mean	feature ID	fold change	FDR Pvalue	ensembl gene id	Prox1 rpkm mean	C57 rpkm mean
Lctl	-190.8	1.7E-13	ENSMUSG00000032401	0.03	2.91	Ndrg1	-11.4	1.4E-16	ENSMUSG00000005125	0.67	5.68
Dnase2b	-73.3	4.4E-11	ENSMUSG00000028185	0.12	5.55	Mafa	-11.3	2.7E-33	ENSMUSG00000047591	1.24	10.27
Birc7	-68.0	2.9E-14	ENSMUSG00000038840	0.14	6.78	Gpr160	-11.1	2.6E-83	ENSMUSG00000037661	1.55	12.93
D630024D03Rik	-64.5	1.4E-10	ENSMUSG00000085772	0.08	3.60	Cryba1	-11.1	3.9E-42	ENSMUSG00000000724	976.24	8287.86
Tmprss11e	-61.6	1.4E-06	ENSMUSG00000054537	0.09	4.03	Ggct	-10.9	2E-26	ENSMUSG00000002797	1.46	12.15
Crygf	-52.6	3.6E-15	ENSMUSG00000025945	92.23	3723.47	1300017J02Rik	-10.7	1.4E-65	ENSMUSG00000033688	1.62	13.03
Bfsp1	-39.2	2.9E-22	ENSMUSG00000027420	18.66	555.71	Tmem179	-10.5	1.6E-09	ENSMUSG00000054013	0.33	2.53
Crygb	-38.7	1.7E-21	ENSMUSG00000073658	276.61	8240.52	Bfsp2	-10.4	4E-26	ENSMUSG00000032556	19.66	155.26
Scn11a	-31.0	8.9E-52	ENSMUSG00000034115	0.15	3.53	Lim2_2	-10.4	9.4E-41	NA	31.34	249.57
Drd4	-30.4	6.5E-76	ENSMUSG00000025496	0.61	12.18	Caprin2	-10.3	7.8E-37	ENSMUSG00000030309	20.60	163.11
Hopx	-25.5	2.3E-22	ENSMUSG00000059325	0.92	17.11	Tmem40	-10.3	6.3E-47	ENSMUSG00000059900	15.31	120.59
Scnn1b	-23.2	2.2E-47	ENSMUSG00000030873	1.53	26.32	Cabp5	-10.2	1.1E-10	ENSMUSG00000005649	0.34	2.56
Gm20757	-23.1	2.9E-14	ENSMUSG00000098040	1.95	33.54	Tmod1	-10.2	1.8E-56	ENSMUSG00000028328	1.79	13.66
Crygd	-21.6	1.3E-31	ENSMUSG00000067299	318.25	5283.50	Fam89a	-10.1	1.5E-33	ENSMUSG00000043068	4.59	34.86
Hspb3	-21.3	5.9E-35	ENSMUSG00000051456	1.24	17.73	B230206L02Rik	-10.0	1.4E-08	ENSMUSG00000086003	0.27	2.09
Sct	-21.2	3.9E-16	ENSMUSG00000038580	0.20	3.35	Dmtn	-9.8	7.7E-54	ENSMUSG00000022099	1.75	12.88
Gm14546	-20.5	3.1E-19	ENSMUSG00000086762	0.17	2.44	Zfp365	-9.8	9E-51	ENSMUSG00000037855	8.10	61.18
Pgam2	-20.3	9.8E-33	ENSMUSG00000020475	11.10	171.23	Crybb3	-9.6	4.8E-42	ENSMUSG00000029352	1301.62	9556.74
Plekhs1	-20.0	6.7E-24	ENSMUSG00000035818	0.44	6.50	Pgm5	-9.6	2E-33	ENSMUSG00000041731	3.00	21.79
Myo18b	-19.6	1.4E-22	ENSMUSG00000072720	0.29	4.23	Scgn	-9.5	1.1E-23	ENSMUSG00000021337	0.69	5.22
Slc24a4	-19.2	1E-28	ENSMUSG00000041771	1.46	21.32	Cela1	-9.3	1.3E-61	ENSMUSG00000023031	10.47	74.85
Gcg	-18.7	4.6E-44	ENSMUSG00000000394	1.45	19.19	Fgfr3	-9.3	3.8E-55	ENSMUSG00000054252	5.26	37.60
Myo7b	-18.2	1.9E-18	ENSMUSG00000024388	0.49	6.71	Hfe	-9.3	8.6E-25	ENSMUSG00000006611	2.12	14.78
Wnt7a	-17.5	1.3E-24	ENSMUSG00000030093	1.31	17.08	Gsn	-9.2	3.9E-45	ENSMUSG00000026879	29.53	210.46
Bcmo1	-16.7	1.9E-25	ENSMUSG00000031845	0.27	3.35	Nol3	-8.9	1.2E-38	ENSMUSG00000014776	1.39	9.21
1700080G11Rik	-16.5	7.7E-10	ENSMUSG00000086771	0.15	2.53	Dync1i1	-8.7	1.4E-20	ENSMUSG00000029757	0.94	6.07
Crygs	-16.0	8E-35	ENSMUSG00000033501	18.08	220.23	Grifin	-8.5	3.8E-51	ENSMUSG00000036586	40.47	263.22
Gm26847	-15.9	8.1E-46	ENSMUSG00000097526	12.78	156.15	Mtnr1a	-8.4	8.9E-32	ENSMUSG00000054764	1.91	12.17
Cryga	-15.8	5.2E-31	ENSMUSG00000044429	1003.75	12221.23	Myh7b	-8.4	8.2E-32	ENSMUSG00000074652	1.23	7.86
St18	-15.7	3.8E-38	ENSMUSG00000033740	0.20	2.22	Gm15417	-8.2	7.2E-09	ENSMUSG00000074466	1.21	7.50
Snx22	-15.6	1E-16	ENSMUSG00000039452	1.12	13.06	Capn3	-8.0	9.8E-56	ENSMUSG00000079110	224.71	1401.46
Cryba2	-15.6	4.9E-46	ENSMUSG00000006546	382.22	4600.10	Gstp2	-7.9	1E-12	ENSMUSG00000038155	1.43	8.34
S100a4	-15.4	6.7E-14	ENSMUSG00000001020	1.68	17.59	Gadd45b	-7.9	6.5E-12	ENSMUSG00000015312	1.29	7.46
Chrng	-15.3	1.9E-41	ENSMUSG00000026253	5.24	61.97	Tdrd7	-7.8	4.5E-42	ENSMUSG00000035517	59.33	354.57
Cryba4	-14.8	5.8E-37	ENSMUSG00000066975	896.00	10270.19	Trpc6	-7.8	2.4E-26	ENSMUSG00000031997	3.36	19.73
Syn2	-14.8	1.9E-57	ENSMUSG00000009394	0.82	8.99	Poln	-7.6	7.5E-13	ENSMUSG00000045102	0.39	2.16
Crygc	-14.6	4.6E-35	ENSMUSG00000025952	340.35	3804.70	Lgi2	-7.5	7.6E-37	ENSMUSG00000039252	6.68	38.45
1500009C09Rik	-13.7	3.7E-33	ENSMUSG00000068099	0.61	5.75	Spta1	-7.5	1.4E-38	ENSMUSG00000026532	0.50	2.88
Prox1os	-13.6	1.1E-48	ENSMUSG00000079045	6.81	70.17	Nrcam	-7.4	2E-38	ENSMUSG00000020598	9.31	53.58
Sec14l5	-13.6	7.6E-37	ENSMUSG00000091712	0.54	4.97	Crygn	-7.4	1.6E-44	ENSMUSG00000038135	535.02	3026.93
Cryge	-13.5	5.1E-38	ENSMUSG00000070870	1025.95	10704.19	Slc46a3	-7.3	3.3E-19	ENSMUSG00000029650	1.52	8.31
Rspo1	-13.5	7.1E-79	ENSMUSG00000028871	4.59	47.02	Akap14	-7.1	5.1E-22	ENSMUSG00000036551	0.93	4.99
Mip	-13.4	7.5E-45	ENSMUSG00000025389	159.97	1657.29	Pip5kl1	-7.0	8E-86	ENSMUSG00000046854	5.34	29.05
Bmper	-12.9	7E-40	ENSMUSG00000031963	4.19	41.69	Unc13c	-7.0	6.6E-19	ENSMUSG00000062151	0.62	3.23
Pla2g7	-12.6	2.9E-24	ENSMUSG00000023913	16.92	162.56	Epn3	-6.9	2.8E-39	ENSMUSG00000010080	0.72	3.83
Ermap	-12.4	1.1E-24	ENSMUSG00000028644	0.71	6.54	Osbp2	-6.8	3.6E-54	ENSMUSG00000020435	6.72	35.42
Lyzl4	-12.3	3.1E-39	ENSMUSG00000032530	1.21	10.96	Tmem252	-6.8	1E-19	ENSMUSG00000048572	1.46	7.40
Gje1	-12.0	2.6E-45	ENSMUSG00000019867	3.93	35.61	Gls2	-6.7	4.1E-22	ENSMUSG00000044005	0.43	2.25
Hsf4	-11.7	1.6E-41	ENSMUSG00000033249	7.13	63.67	Cend1	-6.7	9.8E-25	ENSMUSG00000060240	1.18	5.77
Crybb1	-11.6	8E-49	ENSMUSG00000029343	2318.10	20757.30	Stx11	-6.4	1.7E-05	ENSMUSG00000039232	0.76	3.66

feature ID	fold change	FDR Pvalue	ensembl gene id	Prox1 rpkm mean	C57 rpkm mean	feature ID	fold change	FDR Pvalue	ensembl gene id	Prox1 rpkm mean	C57 rpkm mean
Zbtb7b	-6.5	4.9E-11	ENSMUSG00000028042	2.03	9.93	Fn3krp	-4.9	9E-33	ENSMUSG00000039253	13.59	51.36
Pla2g16	-6.4	1.7E-23	ENSMUSG00000060675	12.55	61.54	Rab42	-4.9	2.9E-09	ENSMUSG00000089687	0.88	3.87
Gm11427	-6.3	3.7E-11	ENSMUSG00000083161	0.54	2.74	Ogn	-4.9	8.4E-13	ENSMUSG00000021390	2.81	10.42
Rsph10b	-6.3	1.4E-12	ENSMUSG00000075569	0.67	3.17	Rnf180	-4.8	6.4E-06	ENSMUSG00000021720	2.50	8.98
Lingo3	-6.2	3.6E-32	ENSMUSG00000051067	0.92	4.47	Prkaa2	-4.7	3.6E-25	ENSMUSG00000028518	2.52	9.12
RP23-380A10.3	-6.2	3.4E-06	NA	0.45	2.00	Hist1h2bc	-4.7	3.8E-35	ENSMUSG00000018102	16.19	58.74
Cryaa	-6.2	4E-42	ENSMUSG00000024041	15055.37	71641.20	Cyb5r2	-4.7	7.1E-12	ENSMUSG00000048065	0.65	2.31
Prkca	-6.2	1.8E-35	ENSMUSG00000050965	1.77	8.31	Rnf19b	-4.7	6.8E-30	ENSMUSG00000028793	10.89	38.89
Pygm	-6.1	2.7E-48	ENSMUSG00000032648	22.49	106.00	Fam46c	-4.6	1.1E-29	ENSMUSG00000044468	25.12	90.13
Thsd4	-6.1	1.3E-11	ENSMUSG00000032289	1.24	5.76	Ace	-4.6	2.5E-22	ENSMUSG00000020681	0.74	2.58
R3hdml	-6.0	2.7E-18	ENSMUSG00000078949	6.20	28.28	Qpct	-4.5	1.6E-22	ENSMUSG00000024084	3.99	13.99
Akr1b8	-6.0	9.3E-22	ENSMUSG00000029762	1.10	5.39	Entpd1	-4.5	4.5E-32	ENSMUSG00000048120	3.85	13.38
Cpeb3	-5.9	6.8E-14	ENSMUSG00000039652	0.46	2.02	Vit	-4.5	9.6E-43	ENSMUSG00000024076	77.18	270.98
Zmat4	-5.9	1.3E-18	ENSMUSG00000037492	0.71	3.15	Ndrg4	-4.5	5.3E-48	ENSMUSG00000036564	4.42	15.31
Kcnma1	-5.8	4.8E-31	ENSMUSG00000063142	0.89	3.86	Tnfrsf23	-4.5	8.6E-20	ENSMUSG00000037613	1.28	4.32
Lin7a	-5.8	1.2E-50	ENSMUSG00000019906	4.10	18.34	Gm11961	-4.5	4.8E-12	ENSMUSG00000056288	1.53	5.39
Rcan2	-5.8	2E-36	ENSMUSG00000039601	2.01	8.75	Pstpip2	-4.5	6E-08	ENSMUSG00000025429	1.27	4.16
Pon2	-5.8	1.1E-38	ENSMUSG00000032667	14.97	66.29	Rgs8	-4.5	3E-51	ENSMUSG00000042671	6.33	21.93
Cd24a	-5.7	1.2E-40	ENSMUSG00000047139	342.95	1517.01	Cnih2	-4.4	9.7E-40	ENSMUSG00000024873	10.49	36.04
Stat5a	-5.7	4.7E-28	ENSMUSG00000004043	0.85	3.65	Gpr19	-4.4	1.2E-37	ENSMUSG00000032641	5.07	17.33
Gm14005	-5.6	4.4E-09	ENSMUSG00000074813	0.62	2.63	Itpk1	-4.4	4E-34	ENSMUSG00000057963	5.66	19.17
Nyap1	-5.5	3.6E-57	ENSMUSG00000045348	11.28	48.42	Itga2	-4.4	1.6E-13	ENSMUSG00000015533	1.69	5.69
Fam131a	-5.5	3.1E-36	ENSMUSG00000050821	3.43	14.48	Gprc5b	-4.4	2.4E-35	ENSMUSG00000008734	19.39	65.84
Add2	-5.4	1.1E-33	ENSMUSG00000030000	5.99	24.93	Fgfrl1	-4.4	2.1E-28	ENSMUSG00000008090	14.83	50.00
Arntl2	-5.4	7.5E-29	ENSMUSG00000040187	1.39	5.68	Dner	-4.4	4.4E-11	ENSMUSG00000036766	1.56	5.17
Espn	-5.3	8.9E-44	ENSMUSG00000028943	1.52	6.18	Sptb	-4.4	1E-19	ENSMUSG00000021061	19.31	65.48
Arhgdig	-5.3	5.3E-23	ENSMUSG00000073433	0.88	3.59	Map6d1	-4.3	1E-27	ENSMUSG00000041205	2.53	8.41
Ptgfr	-5.3	8.1E-17	ENSMUSG00000028036	2.54	10.28	Dbnl	-4.3	1E-36	ENSMUSG00000020476	59.24	198.23
Htatip2	-5.3	6.7E-10	ENSMUSG00000039745	0.74	2.71	Jazf1	-4.3	1E-52	ENSMUSG00000063568	6.48	21.77
Efcab10	-5.2	3.3E-06	ENSMUSG00000020562	0.58	2.58	S1pr5	-4.3	1.5E-17	ENSMUSG00000045087	1.32	4.35
2900005J15Rik	-5.2	1.1E-11	ENSMUSG00000043833	0.78	3.21	Btbd17	-4.3	7.7E-40	ENSMUSG00000000202	5.19	17.26
B230312C02Rik	-5.2	4.4E-42	ENSMUSG00000084843	7.32	29.36	Hist2h3c2	-4.2	1.1E-09	ENSMUSG00000081058	1.12	3.51
Gm17586	-5.2	2E-32	ENSMUSG00000097062	18.44	73.00	Magi2_1	-4.2	1.1E-07	NA	0.77	2.46
Gja3	-5.2	5.5E-38	ENSMUSG00000048582	69.21	274.68	Tex2	-4.2	8.8E-26	ENSMUSG00000040548	5.42	17.49
Lsamp	-5.1	3.7E-22	ENSMUSG00000061080	1.08	4.28	Snhg12	-4.2	1.6E-17	ENSMUSG00000086290	21.58	68.97
Gss	-5.1	3.4E-30	ENSMUSG00000027610	6.90	27.08	Adc	-4.2	1.1E-20	ENSMUSG00000028789	3.64	11.57
Zfp185	-5.1	1.1E-49	ENSMUSG00000031351	12.06	47.51	Tob1	-4.1	3.2E-24	ENSMUSG00000037573	39.37	125.10
Nkg7	-5.1	2.7E-08	ENSMUSG00000004612	0.52	2.11	Cdkl2	-4.1	2.8E-20	ENSMUSG00000029403	0.98	3.07
Mboat1	-5.0	4.9E-41	ENSMUSG00000038732	11.52	44.52	Abtb2	-4.1	3E-19	ENSMUSG00000032724	3.73	11.59
Rnaset2b	-5.0	1.3E-23	ENSMUSG00000094724	1.80	6.87	Reep1	-4.0	4.6E-37	ENSMUSG00000052852	12.02	37.56
Paqr7	-5.0	6.9E-31	ENSMUSG00000037348	2.00	7.67	Adra2a	-4.0	4.9E-19	ENSMUSG00000033717	0.91	2.78
Synm	-5.0	9.5E-23	ENSMUSG00000030554	10.57	40.79	Metap1	-4.0	2.3E-29	ENSMUSG00000005813	33.44	103.99
Gstp1	-5.0	5.5E-30	ENSMUSG00000060803	52.86	202.87	Optn	-4.0	1.4E-10	ENSMUSG00000026672	4.45	13.59
Clgn	-5.0	9.2E-31	ENSMUSG00000002190	1.24	4.76	Tecrl	-4.0	3.5E-07	ENSMUSG00000049537	0.85	2.66
Sqrdl	-5.0	1.9E-27	ENSMUSG00000005803	1.21	4.57	Stk39	-4.0	1.3E-36	ENSMUSG00000027030	19.00	59.09
Sorbs1	-5.0	2.1E-20	ENSMUSG00000025006	4.65	17.79	Fam46b	-4.0	0.00012	ENSMUSG00000046694	0.84	2.54
Aldoc	-5.0	3.6E-28	ENSMUSG00000017390	2.27	8.52	Kif1a	-4.0	1.3E-13	ENSMUSG00000014602	14.51	44.61
Hebp2	-5.0	1.9E-44	ENSMUSG00000019853	5.02	19.03	Pmp22	-4.0	1.1E-27	ENSMUSG00000018217	24.44	74.78
Wnt7b	-5.0	4.7E-22	ENSMUSG00000022382	13.42	50.96	Cyyr1	-4.0	1.2E-16	ENSMUSG00000041134	4.04	12.34
Metrnl	-4.9	1E-35	ENSMUSG00000039208	7.34	27.71	Clu	-3.9	1.9E-23	ENSMUSG00000022037	30.72	93.71

feature ID	fold change	FDR Pvalue	ensembl gene id	Prox1 rpkm mean	C57 rpkm mean	feature ID	fold change	FDR Pvalue	ensembl gene id	Prox1 rpkm mean	C57 rpkm mean
Ctnna2	-3.9	4E-42	ENSMUSG00000063063	2.34	7.13	Arvcf	-3.2	4E-24	ENSMUSG00000000325	19.17	46.55
Id2	-3.9	3.7E-45	ENSMUSG00000020644	60.12	183.57	Kcnq4	-3.2	1.3E-25	ENSMUSG00000028631	2.52	6.09
Gck	-3.9	2.5E-36	ENSMUSG00000041798	5.95	18.14	Adamts18	-3.2	5.5E-29	ENSMUSG00000053399	22.87	56.15
Vwa5a	-3.9	3E-24	ENSMUSG00000023186	9.90	29.97	Tmem9b	-3.2	4.1E-25	ENSMUSG00000031021	17.04	41.75
Gpr137b-ps	-3.9	5.9E-11	ENSMUSG00000097715	1.28	3.72	Rpl34	-3.2	6.2E-06	ENSMUSG00000062006	35.79	87.59
Mturn	-3.9	4.4E-25	ENSMUSG00000038065	7.59	22.69	Blvra	-3.1	3.3E-14	ENSMUSG00000001999	2.81	6.74
Casp7	-3.9	8.4E-19	ENSMUSG00000025076	14.37	42.48	B3gnt5	-3.1	5.6E-22	ENSMUSG00000022686	19.42	46.86
Tppp3	-3.9	7.4E-39	ENSMUSG00000014846	7.65	22.95	Tbc1d22a	-3.1	1.6E-18	ENSMUSG00000051864	10.67	25.51
Rnf113a1	-3.8	4.8E-09	ENSMUSG00000036537	25.74	74.72	Gm11837	-3.1	1.3E-10	ENSMUSG00000086587	5.76	13.68
Dock5	-3.8	5E-19	ENSMUSG00000044447	9.10	27.10	Adamtsl4	-3.1	8.2E-09	ENSMUSG00000015850	3.07	7.23
Ndufs5	-3.8	9.2E-13	ENSMUSG00000028648	4.74	13.92	Cars	-3.1	4.7E-20	ENSMUSG00000010755	13.63	32.32
Il18	-3.8	5.7E-08	ENSMUSG00000039217	1.47	4.41	Slain1	-3.1	2.5E-31	ENSMUSG00000055717	6.06	14.59
Fibin	-3.7	0.0001	ENSMUSG00000074971	2.05	5.80	Gpr137b	-3.1	2.1E-22	ENSMUSG00000021306	46.74	110.92
Mocs2	-3.7	1E-23	ENSMUSG00000015536	8.37	23.91	Nudt22	-3.1	1.4E-15	ENSMUSG00000037349	7.39	17.53
Tsc2	-3.7	2.5E-15	ENSMUSG00000002496	22.41	63.47	Rexo2	-3.0	2.8E-21	ENSMUSG00000032026	35.97	84.09
Syt5	-3.7	7E-12	ENSMUSG00000004961	1.82	5.08	Gm14295	-3.0	1E-10	ENSMUSG00000078877	1.12	2.63
Prkag2	-3.7	1.8E-32	ENSMUSG00000028944	6.96	19.74	Fgfbp3	-3.0	7.7E-14	ENSMUSG00000047632	5.43	12.72
Rfx8	-3.7	5.8E-09	ENSMUSG00000057173	0.83	2.26	Rasl11b	-3.0	1.5E-25	ENSMUSG00000049907	54.36	126.61
Sptbn1	-3.7	1.4E-19	ENSMUSG00000020315	32.36	92.67	Kif26b	-3.0	0.00017	ENSMUSG00000026494	0.96	2.22
Rilpl1	-3.7	1E-35	ENSMUSG00000029392	28.59	81.06	Ddx26b	-3.0	1.2E-20	ENSMUSG00000035967	32.33	74.76
Kcnj11	-3.6	9.5E-12	ENSMUSG00000096146	2.65	7.43	Lnp	-3.0	2.1E-19	ENSMUSG00000009207	7.04	16.12
Serpinb6b	-3.6	1.8E-08	ENSMUSG00000042842	0.95	2.59	Cttnbp2	-3.0	1.2E-19	ENSMUSG00000000416	2.17	4.95
Tubb2a	-3.6	3.7E-31	ENSMUSG00000058672	17.02	47.80	Hlcs	-3.0	1.7E-25	ENSMUSG00000040820	9.44	21.66
Efcab1	-3.6	1.5E-35	ENSMUSG00000068617	12.03	33.77	Pnpla6	-2.9	1.3E-39	ENSMUSG00000004565	9.58	21.92
Abcc8	-3.6	1.7E-28	ENSMUSG00000040136	3.22	9.07	Cbs	-2.9	2.5E-11	ENSMUSG00000024039	0.88	2.03
Gpm6b	-3.6	3.6E-14	ENSMUSG00000031342	4.88	13.42	Sntb1	-2.9	3E-11	ENSMUSG00000060429	6.46	14.50
Cpne7	-3.6	6.8E-16	ENSMUSG00000034796	0.97	2.71	Pbx4	-2.9	2.4E-14	ENSMUSG00000031860	2.34	5.40
Nap1l4	-3.6	2E-31	ENSMUSG00000059119	236.18	653.88	Adam9	-2.9	1.1E-25	ENSMUSG00000031555	20.73	46.22
Gadd45g	-3.5	6E-13	ENSMUSG00000021453	9.36	25.26	Gas6	-2.9	1.6E-16	ENSMUSG00000031451	8.10	17.78
Cpeb2	-3.5	4.3E-23	ENSMUSG00000039782	5.21	14.14	Ppip5k2	-2.9	8.1E-28	ENSMUSG00000040648	8.31	18.41
Map6	-3.5	3.7E-43	ENSMUSG00000055407	6.19	16.82	Zfp385a	-2.8	6E-32	ENSMUSG00000000552	34.12	75.71
Osbpl11	-3.5	7.5E-29	ENSMUSG00000022807	14.83	39.87	Insig1	-2.8	2.8E-28	ENSMUSG00000045294	31.09	68.61
Ptplad2	-3.5	1.2E-24	ENSMUSG00000028497	4.69	12.53	Igsf9	-2.8	2.4E-21	ENSMUSG00000037995	18.84	41.24
Cpeb1	-3.4	4.5E-34	ENSMUSG00000025586	6.15	16.32	Nabp1	-2.8	2.9E-14	ENSMUSG00000026107	2.85	6.22
Bpnt1	-3.4	2.3E-43	ENSMUSG00000026617	14.22	37.85	Peli1	-2.8	4.1E-24	ENSMUSG00000020134	13.36	29.19
Dgkg	-3.4	1.8E-10	ENSMUSG00000022861	0.80	2.06	E530001K10Rik	-2.8	6.2E-08	ENSMUSG00000075020	4.82	10.40
Ell2	-3.4	1.7E-26	ENSMUSG00000001542	52.22	137.46	Gls	-2.8	2.6E-21	ENSMUSG00000026103	12.27	26.70
Atp8a1	-3.4	1.6E-14	ENSMUSG00000037685	1.48	3.87	Gm13152	-2.8	6.3E-09	ENSMUSG00000078496	4.28	9.30
Pde2a	-3.3	6.3E-11	ENSMUSG00000030653	8.34	21.23	Gm5607	-2.8	4.7E-19	ENSMUSG00000047935	7.36	15.96
Fxyd1	-3.3	2.6E-08	ENSMUSG00000036570	2.85	7.36	Aldh1a7	-2.8	7.2E-20	ENSMUSG00000024747	40.36	87.36
Dnmbp	-3.3	7.8E-20	ENSMUSG00000025195	9.66	24.52	Snap91	-2.8	1.6E-19	ENSMUSG00000033419	2.08	4.50
Nexn	-3.3	1.2E-18	ENSMUSG00000039103	3.19	8.08	Sardh	-2.8	6.8E-07	ENSMUSG00000009614	1.01	2.16
Ngef	-3.3	4.5E-30	ENSMUSG00000026259	4.55	11.50	C2cd2l	-2.8	5.8E-29	ENSMUSG00000032120	5.37	11.66
Herc4	-3.2	2.7E-28	ENSMUSG00000020064	32.19	80.77	Scamp5	-2.8	1.6E-11	ENSMUSG00000040722	7.57	16.15
Rnf123	-3.2	8.6E-27	ENSMUSG00000041528	6.21	15.53	Megf9	-2.8	6E-14	ENSMUSG00000039270	15.45	33.12
Lyrm1	-3.2	2.2E-12	ENSMUSG00000030922	2.48	6.24	Dnajb2	-2.8	3.6E-18	ENSMUSG00000026203	9.49	20.34
Pdlim1	-3.2	1.7E-13	ENSMUSG00000055044	3.32	8.13	Hmgn3	-2.8	6.4E-11	ENSMUSG00000066456	34.04	72.23
Rab3b	-3.2	1.8E-19	ENSMUSG00000003411	2.55	6.33	Mecr	-2.8	2.9E-22	ENSMUSG00000028910	7.13	15.31
Rnaset2a	-3.2	9.7E-09	ENSMUSG00000095687	1.61	4.06	Sowaha	-2.8	7.6E-22	ENSMUSG00000044352	14.99	32.44
Nacc2	-3.2	2E-16	ENSMUSG00000026932	2.08	5.07	Mob3b	-2.8	1.2E-16	ENSMUSG00000073910	3.08	6.54

feature ID	fold change	FDR Pvalue	ensembl gene id	Prox1 rpkm mean	C57 rpkm mean	feature ID	fold change	FDR Pvalue	ensembl gene id	Prox1 rpkm mean	C57 rpkm mean
Sptan1	-2.8	4.7E-22	ENSMUSG00000057738	65.64	140.46	Mettl22	-2.6	3.2E-13	ENSMUSG00000039345	3.10	6.24
Dst	-2.7	1.6E-06	ENSMUSG00000026131	6.80	14.68	Ncoa7	-2.6	1.8E-15	ENSMUSG00000039697	7.08	14.23
Efcab2	-2.7	2.7E-14	ENSMUSG00000026495	5.04	10.57	C77080	-2.6	1.4E-20	ENSMUSG00000050390	8.67	17.45
Klhl5	-2.7	4.5E-20	ENSMUSG00000054920	5.85	12.29	Rbp3	-2.6	7.9E-13	ENSMUSG00000041534	5.42	10.79
Zbtb8b	-2.7	1.3E-24	ENSMUSG00000048485	7.08	15.03	Spg20	-2.6	1.1E-22	ENSMUSG00000036580	19.89	39.91
Ipo8	-2.7	2.2E-22	ENSMUSG00000040029	9.64	20.52	Slc25a22	-2.6	1.2E-11	ENSMUSG00000019082	4.38	8.76
Reep2	-2.7	1.8E-28	ENSMUSG00000038555	12.41	26.31	Trim9	-2.6	1.3E-23	ENSMUSG00000021071	5.85	11.71
Kcnj12	-2.7	2.9E-24	ENSMUSG00000042529	10.15	21.47	Eno3	-2.6	3.7E-25	ENSMUSG00000060600	23.84	47.99
Prx	-2.7	6.6E-18	ENSMUSG00000053198	13.87	29.09	Tubb6	-2.6	2.4E-22	ENSMUSG00000001473	32.95	65.97
Fah	-2.7	8.3E-09	ENSMUSG00000030630	1.35	2.87	Mllt11	-2.6	6.2E-08	ENSMUSG00000053192	2.64	5.22
Nedd4l	-2.7	3.3E-19	ENSMUSG00000024589	2.52	5.28	9930104L06Rik	-2.6	7.9E-20	ENSMUSG00000044730	3.71	7.41
Vldlr	-2.7	2.3E-17	ENSMUSG00000024924	7.24	15.08	Gm14296	-2.6	8E-17	ENSMUSG00000074527	2.04	4.06
Cpt2	-2.7	5.7E-17	ENSMUSG00000028607	15.80	32.74	Spink13	-2.6	0.01804	ENSMUSG00000073551	2.41	4.69
Prkab2	-2.7	2.5E-15	ENSMUSG00000038205	7.45	15.35	Epb4.1l4a	-2.6	5.3E-22	ENSMUSG00000024376	40.29	79.89
Pcsk6	-2.7	3.6E-08	ENSMUSG00000030513	1.74	3.53	Rhot1	-2.6	5.2E-15	ENSMUSG00000017686	8.28	16.29
Ass1	-2.7	5.1E-14	ENSMUSG00000076441	4.36	8.88	Osgin2	-2.6	3.9E-17	ENSMUSG00000041153	4.46	8.83
Cyp7b1	-2.7	1E-10	ENSMUSG00000039519	3.00	6.14	Dnajb1	-2.6	5E-10	ENSMUSG00000005483	28.72	56.13
Mthfd1l	-2.6	1.5E-27	ENSMUSG00000040675	14.37	29.63	Slc38a5	-2.5	5.8E-06	ENSMUSG00000031170	1.02	2.05
Gpx1	-2.6	8.9E-19	ENSMUSG00000063856	165.58	337.66	Mapk8ip1	-2.5	4.3E-24	ENSMUSG00000027223	8.88	17.51
Uchl1	-2.6	4.1E-18	ENSMUSG00000029223	57.91	117.93	Fktn	-2.5	9.6E-19	ENSMUSG00000028414	11.92	23.47
Eif2s3y	-2.6	1.4E-06	ENSMUSG00000069049	6.74	13.57	Inf2	-2.5	4.8E-07	ENSMUSG00000037679	1.74	3.36
A430105I19Rik	-2.6	2.3E-23	ENSMUSG00000045838	4.80	9.77	Tdrkh	-2.5	2.9E-21	ENSMUSG00000041912	11.96	23.48
Spag5	-2.6	4.2E-23	ENSMUSG00000002055	17.91	36.48	Pkp2	-2.5	2.7E-27	ENSMUSG00000041957	7.07	13.91
Cul3	-2.6	1.4E-22	ENSMUSG00000004364	52.92	107.96	Kat2b	-2.5	3.3E-14	ENSMUSG00000000708	4.50	8.76
Nudt17	-2.6	3.1E-06	ENSMUSG00000028100	1.18	2.50	Gabrg3	-2.5	3.2E-06	ENSMUSG00000055026	1.06	2.03
Me1	-2.6	2.4E-15	ENSMUSG00000032418	4.99	10.06	Mthfsl	-2.5	7.9E-07	ENSMUSG00000079427	1.19	2.36
Zfyve21	-2.6	1.6E-21	ENSMUSG00000021286	19.62	39.89	Dpf3	-2.5	2.1E-08	ENSMUSG00000021221	2.28	4.37
Gm14326	-2.6	2.6E-05	ENSMUSG00000078862	1.34	2.65	Arhgap31	-2.5	2.8E-07	ENSMUSG00000022799	7.33	14.35

Development • Supplementary information

Supplementary Table 4: Genes up-regulated following Prox1 loss

feature ID	fold change	FDR Pvalue	ensembl gene id	Prox1 mean RPKM	C57 mean RPKM	feature ID	fold change	FDR Pvalue	ensembl gene id	Prox1 mean RPKM	C57 mean RPKM
Calb1	120.5	1.1E-124	ENSMUSG00000028222	11.89	0.08	Lox	5.4	2.1E-04	ENSMUSG00000024529	13.32	1.98
Ppp1r14c	67.6	1.4E-77	ENSMUSG00000040653	12.28	0.14	Mrc2	5.3	2.1E-24	ENSMUSG00000020695	21.66	3.24
Cngb3	55.9	2.3E-159	ENSMUSG00000056494	18.91	0.26	Gfra2	5.3	2.4E-34	ENSMUSG00000022103	13.70	2.02
Pde11a	49.5	2.0E-34	ENSMUSG00000075270	2.01	0.03	Gm11650	5.3	2.6E-07	ENSMUSG00000087184	2.23	0.33
Tnc	30.6	1.2E-82	ENSMUSG00000028364	55.12	1.40	Slc22a5	5.2	3.4E-35	ENSMUSG00000018900	14.78	2.21
Hpse	27.0	9.7E-82	ENSMUSG00000035273	11.58	0.33	Kera	5.2	2.6E-03	ENSMUSG00000019932	8.77	1.26
Rgs6	20.8	7.3E-76	ENSMUSG00000021219	5.46	0.21	Rgs13	5.2	6.3E-14	ENSMUSG00000051079	15.63	2.33
Gm12901	18.6	2.0E-02	ENSMUSG00000083720	22.89	0.93	Glb1l2	5.2	3.7E-27	ENSMUSG00000036395	4.35	0.65
Sox21	18.4	3.8E-34	ENSMUSG00000061517	3.51	0.15	Elmod1	5.2	1.2E-13	ENSMUSG00000041986	3.17	0.48
C1qtnf4	18.1	3.9E-45	ENSMUSG00000040794	21.80	0.94	Krt5	5.2	3.3E-04	ENSMUSG00000061527	15.57	2.42
Prokr1	13.4	1.6E-60	ENSMUSG00000049409	26.03	1.51	Klhl14	5.2	1.8E-20	ENSMUSG00000042514	4.10	0.62
Klf5	12.7	4.4E-10	ENSMUSG00000005148	2.05	0.12	Gm21738	5.2	3.8E-02	ENSMUSG00000095280	43.94	7.16
Tlr5	12.5	9.9E-23	ENSMUSG00000079164	2.11	0.13	Slc11a1	5.1	1.0E-18	ENSMUSG00000026177	5.44	0.84
Slc1a2	12.0	1.5E-78	ENSMUSG00000005089	7.35	0.48	Kcna5	5.0	3.3E-11	ENSMUSG00000045534	7.30	1.16
Tff2	11.9	2.7E-11	ENSMUSG00000024028	5.02	0.33	4930426D05Rik	5.0	1.1E-09	ENSMUSG00000043168	3.46	0.54
Slc44a5	11.5	8.0E-49	ENSMUSG00000028360	4.76	0.33	Smoc2	5.0	7.1E-04	ENSMUSG00000023886	8.17	1.27
Gm5900	10.5	5.5E-11	ENSMUSG00000094685	3.23	0.24	Vcan	4.9	4.3E-15	ENSMUSG00000021614	18.68	3.04
Ttr	10.2	2.7E-03	ENSMUSG00000061808	5.00	0.40	Col17a1	4.8	9.6E-04	ENSMUSG00000025064	2.32	0.39
Trac	10.1	3.0E-07	ENSMUSG00000076928	2.70	0.19	Pdgfc	4.7	7.0E-13	ENSMUSG00000028019	6.07	1.02
Gm15631	10.0	7.5E-11	ENSMUSG00000085067	3.08	0.24	Bves	4.7	4.8E-18	ENSMUSG00000071317	6.48	1.07
Pxdc1	8.5	1.4E-30	ENSMUSG00000021411	10.77	0.99	Ahnak	4.7	2.6E-06	ENSMUSG00000069833	10.79	1.86
Smim1	7.9	3.9E-45	ENSMUSG00000078350	5.10	0.51	Nkain4	4.7	5.9E-17	ENSMUSG00000027574	10.71	1.79
Tnnt3	7.7	5.7E-15	ENSMUSG00000061723	3.82	0.38	Matn4	4.7	7.7E-03	ENSMUSG00000016995	4.47	0.74
Cxcl14	7.7	2.0E-17	ENSMUSG00000021508	4.21	0.42	Ramp3	4.6	4.0E-17	ENSMUSG00000041046	6.87	1.16
Cma1	7.7	3.5E-07	ENSMUSG00000022225	2.03	0.21	Lypd6b	4.6	3.5E-13	ENSMUSG00000026765	4.15	0.70
Depdc7	7.6	3.4E-15	ENSMUSG00000027173	2.43	0.25	Cx3cl1	4.6	2.2E-43	ENSMUSG00000031778	94.65	15.90
Capn6	7.6	2.0E-17	ENSMUSG00000067276	11.99	1.26	Tyr	4.5	3.5E-05	ENSMUSG00000004651	15.38	2.73
Ppfibp2	7.5	1.1E-44	ENSMUSG00000036528	10.21	1.08	Klhdc8a	4.5	7.5E-13	ENSMUSG00000042115	2.68	0.46
Wfikkn2	7.2	6.7E-35	ENSMUSG00000044177	5.88	0.63	Nfix	4.5	2.9E-04	ENSMUSG00000001911	2.30	0.41
Pltp	7.2	4.6E-15	ENSMUSG00000017754	11.76	1.30	Osbpl3	4.4	8.6E-46	ENSMUSG00000029822	12.89	2.28
Trim6	7.2	3.5E-25	ENSMUSG00000072244	8.35	0.91	Hist1h1d	4.4	1.2E-03	ENSMUSG00000052565	4.88	0.86
Krt15	7.1	3.3E-05	ENSMUSG00000054146	8.79	0.97	Sox9	4.4	8.8E-28	ENSMUSG00000000567	12.97	2.31
Srpx	6.6	2.1E-22	ENSMUSG00000090084	5.70	0.67	Rlbp1	4.4	9.0E-07	ENSMUSG00000039194	8.25	1.50
Gm10800	6.4	1.2E-02	ENSMUSG00000075014	956.81	124.16	Dsp	4.4	1.0E-04	ENSMUSG00000054889	3.32	0.61
Itga8	6.4	2.8E-21	ENSMUSG00000026768	3.40	0.42	Cldn11	4.4	1.3E-04	ENSMUSG00000037625	4.01	0.72
Eln	6.4	5.4E-04	ENSMUSG00000029675	9.16	1.13	Egfl6	4.4	1.1E-03	ENSMUSG00000000402	3.86	0.69
Phactr1	6.2	1.2E-21	ENSMUSG00000054728	2.52	0.32	Col8a1	4.3	6.0E-04	ENSMUSG00000068196	8.19	1.53
Tifa	6.2	2.1E-23	ENSMUSG00000046688	10.42	1.31	Col12a1	4.3	5.2E-04	ENSMUSG00000032332	10.04	1.89
Tshr	6.2	8.4E-23	ENSMUSG00000020963	5.02	0.64	Agtr2	4.3	4.8E-03	ENSMUSG00000068122	7.46	1.38
Gm10801	6.1	1.2E-02	ENSMUSG00000075015	269.14	36.60	Fras1	4.3	7.3E-14	ENSMUSG00000034687	9.69	1.80
Col1a1	6.1	1.2E-05	ENSMUSG00000001506	102.48	13.25	Dusp4	4.3	3.2E-29	ENSMUSG00000031530	20.67	3.72
Mapk4	6.1	1.3E-37	ENSMUSG00000024558	5.85	0.75	Frem1	4.3	3.2E-08	ENSMUSG00000059049	2.28	0.42
Nnat	5.6	1.2E-53	ENSMUSG00000067786	40.59	5.63	Kitl	4.3	3.5E-23	ENSMUSG00000019966	19.30	3.60
Nrg1	5.6	3.6E-12	ENSMUSG00000062991	3.63	0.51	Abcc4	4.2	9.6E-33	ENSMUSG00000032849	20.38	3.78
Col14a1	5.6	2.8E-04	ENSMUSG00000022371	6.36	0.90	Clec11a	4.2	1.4E-12	ENSMUSG00000004473	3.71	0.69
A930003A15Rik	5.6	6.2E-27	ENSMUSG00000075330	53.49	7.37	Crb1	4.2	6.6E-12	ENSMUSG00000063681	2.40	0.44
Fosl2	5.5	5.2E-22	ENSMUSG00000029135	4.29	0.61	Slc4a5	4.2	1.6E-04	ENSMUSG00000068323	8.44	1.61
Gprc5a	5.5	1.3E-14	ENSMUSG00000046733	3.58	0.51	Sema3c	4.2	3.0E-04	ENSMUSG00000028780	2.74	0.51
Pdlim3	5.5	3.5E-10	ENSMUSG00000031636	3.84	0.54	Fam46a	4.2	2.0E-09	ENSMUSG00000032265	4.50	0.84
Sytl2	5.5	2.6E-17	ENSMUSG00000030616	2.21	0.32	Ndnf	4.1	2.2E-16	ENSMUSG00000049001	13.13	2.53

feature ID	fold change	FDR Pvalue	ensembl gene id	Prox1 mean RPKM	C57 mean RPKM	feature ID	fold change	FDR Pvalue	ensembl gene id	Prox1 mean RPKM	C57 mean RPKM
Fam46a	4.2	2.0E-09	ENSMUSG00000032265	4.50	0.84	Edaradd	3.4	9.5E-19	ENSMUSG00000095105	11.46	2.63
Ndnf	4.1	2.2E-16	ENSMUSG00000049001	13.13	2.53	Dct	3.4	3.8E-04	ENSMUSG00000022129	43.86	10.43
Papss2	4.1	4.1E-12	ENSMUSG00000024899	4.68	0.90	Slc45a2	3.4	7.6E-04	ENSMUSG00000022243	2.58	0.61
Hist1h1b	4.1	1.6E-02	ENSMUSG00000058773	7.35	1.44	Cacna1g	3.4	1.7E-04	ENSMUSG00000020866	3.77	0.90
Asic2	4.1	6.3E-12	ENSMUSG00000020704	2.55	0.49	Tmem144	3.4	6.8E-07	ENSMUSG00000027956	2.56	0.60
Spp1	4.0	6.5E-08	ENSMUSG00000029304	10.54	2.03	Bace2	3.3	1.3E-04	ENSMUSG00000040605	3.51	0.83
Kdelr3	4.0	4.3E-08	ENSMUSG00000010830	6.36	1.24	Plxnc1	3.3	2.1E-17	ENSMUSG00000074785	7.03	1.67
Osr2	4.0	3.1E-02	ENSMUSG00000022330	2.86	0.57	Hs3st5	3.3	3.2E-12	ENSMUSG00000044499	2.48	0.58
Postn	3.9	1.1E-04	ENSMUSG00000027750	8.06	1.63	Col8a2	3.3	2.1E-04	ENSMUSG00000056174	15.05	3.61
Dab2	3.9	2.6E-21	ENSMUSG00000022150	12.26	2.48	Creb3l1	3.3	4.8E-04	ENSMUSG00000027230	3.89	0.93
Npr3	3.9	3.8E-15	ENSMUSG00000022206	13.31	2.74	Tmem169	3.3	7.7E-09	ENSMUSG00000026188	2.61	0.62
Clec14a	3.9	3.1E-25	ENSMUSG00000045930	12.31	2.49	Frk	3.3	8.6E-07	ENSMUSG00000019779	2.20	0.52
Tspan10	3.8	1.1E-05	ENSMUSG00000039691	10.15	2.10	Nid2	3.3	4.7E-17	ENSMUSG00000021806	42.06	10.28
Fbln5	3.8	2.3E-03	ENSMUSG00000021186	3.14	0.65	Pqlc2	3.3	1.1E-14	ENSMUSG00000028744	5.50	1.32
Col6a1	3.8	1.4E-04	ENSMUSG00000001119	17.74	3.68	Aass	3.3	2.7E-09	ENSMUSG00000029695	3.16	0.77
Aqp4	3.8	1.1E-11	ENSMUSG00000024411	2.65	0.54	Igsf3	3.2	6.5E-26	ENSMUSG00000042035	22.18	5.36
Acta2	3.8	1.6E-29	ENSMUSG00000035783	20.86	4.27	Mlana	3.2	4.5E-05	ENSMUSG00000024806	16.25	3.97
Lpcat2	3.8	9.0E-12	ENSMUSG00000033192	2.79	0.58	Krt19	3.2	1.4E-03	ENSMUSG00000020911	2.77	0.67
Col16a1	3.8	2.2E-04	ENSMUSG00000040690	3.22	0.68	Pdgfrl	3.2	9.9E-06	ENSMUSG00000031595	2.27	0.54
Dcn	3.7	2.9E-05	ENSMUSG00000019929	37.46	7.82	4932443I19Rik	3.2	7.5E-05	ENSMUSG00000090336	2.78	0.68
Col6a2	3.7	3.8E-04	ENSMUSG00000020241	9.32	1.98	Myof	3.2	3.0E-05	ENSMUSG00000048612	2.12	0.52
Pmel	3.7	3.0E-04	ENSMUSG00000025359	126.72	27.29	Sfrp2	3.2	2.3E-16	ENSMUSG00000027996	662.84	164.28
Col1a2	3.7	3.6E-05	ENSMUSG00000029661	49.37	10.60	2010107G23Rik	3.2	2.3E-15	ENSMUSG00000020083	8.35	2.06
Apoc1	3.7	9.0E-04	ENSMUSG00000040564	2.22	0.45	Satb2	3.2	5.3E-11	ENSMUSG00000038331	2.03	0.50
Wnt6	3.7	4.1E-02	ENSMUSG00000033227	3.12	0.69	Cdh3	3.2	1.9E-04	ENSMUSG00000061048	6.39	1.61
Kctd12b	3.7	3.2E-21	ENSMUSG00000041633	13.89	3.00	Cacng4	3.2	1.4E-33	ENSMUSG00000020723	31.51	7.82
Tnik	3.7	1.1E-25	ENSMUSG00000027692	3.83	0.81	Prrx1	3.2	1.1E-04	ENSMUSG00000026586	5.04	1.28
Tgfbi	3.6	5.7E-05	ENSMUSG00000035493	9.09	1.99	Tmem35	3.1	2.0E-17	ENSMUSG00000033578	40.16	9.87
Gli1	3.6	5.6E-09	ENSMUSG00000025407	7.53	1.62	Fjx1	3.1	6.5E-30	ENSMUSG00000075012	29.87	7.43
Enc1	3.6	1.6E-30	ENSMUSG00000041773	22.17	4.83	Emp2	3.1	6.7E-10	ENSMUSG00000022505	2.83	0.71
Slc7a7	3.6	2.2E-24	ENSMUSG00000000958	26.13	5.62	Flnc	3.1	2.8E-04	ENSMUSG00000068699	3.75	0.98
Pipox	3.6	8.8E-10	ENSMUSG00000017453	5.95	1.27	Nfia	3.1	8.9E-06	ENSMUSG00000028565	4.13	1.07
Gpnmb	3.6	8.0E-05	ENSMUSG00000029816	16.18	3.59	Vcam1	3.1	1.5E-03	ENSMUSG00000027962	5.64	1.45
Slc24a5	3.6	2.1E-04	ENSMUSG00000035183	4.03	0.89	Mmp14	3.1	3.5E-20	ENSMUSG00000000957	62.64	16.14
Trp53i11	3.6	3.1E-21	ENSMUSG00000068735	28.17	6.25	Tril	3.1	1.8E-06	ENSMUSG00000043496	13.10	3.43
Tyrp1	3.5	3.9E-04	ENSMUSG00000005994	16.22	3.65	Anpep	3.1	6.4E-05	ENSMUSG00000039062	2.69	0.69
Slc6a11	3.5	4.5E-20	ENSMUSG00000030307	11.66	2.53	Sema3f	3.1	1.2E-22	ENSMUSG00000034684	20.57	5.28
Zfhx3	3.5	8.6E-07	ENSMUSG00000038872	12.64	2.88	Sncaip	3.1	6.1E-04	ENSMUSG00000024534	3.07	0.80
Fat3	3.5	1.1E-11	ENSMUSG00000074505	10.32	2.32	Egfem1	3.1	8.2E-21	ENSMUSG00000063600	20.82	5.31
Fst	3.5	5.9E-09	ENSMUSG00000021765	8.80	1.98	Slc35d3	3.1	1.1E-04	ENSMUSG00000050473	2.21	0.56
Lrrn2	3.5	1.2E-15	ENSMUSG00000026443	5.71	1.27	Tmem119	3.1	9.7E-04	ENSMUSG00000054675	5.63	1.47
Pex5l	3.5	1.2E-13	ENSMUSG00000027674	2.40	0.54	Lars2	3.1	6.0E-03	ENSMUSG00000035202	11537.92	3080.25
Cpa3	3.5	6.7E-05	ENSMUSG00000001865	4.20	0.95	Pcdh9	3.1	5.5E-05	ENSMUSG00000055421	2.60	0.67
Igfbp2	3.5	2.4E-15	ENSMUSG00000039323	118.60	26.93	Tst	3.1	2.4E-18	ENSMUSG00000044986	24.53	6.29
Steap4	3.5	2.2E-07	ENSMUSG00000012428	4.25	0.96	Cd44	3.1	2.4E-03	ENSMUSG00000005087	2.66	0.69
Wisp1	3.5	4.8E-03	ENSMUSG00000005124	2.08	0.48	Hs3st6	3.1	6.6E-07	ENSMUSG00000039628	6.10	1.58
Rab32	3.4	4.9E-12	ENSMUSG00000019832	9.94	2.26	Slc38a8	3.0	2.6E-03	ENSMUSG00000034224	21.71	5.79
Jam2	3.4	5.2E-35	ENSMUSG00000053062	9.86	2.24	Igf1	3.0	3.5E-05	ENSMUSG00000020053	4.18	1.12
Zfp462	3.4	2.9E-14	ENSMUSG00000060206	20.46	4.80						

feature ID	fold change	FDR Pvalue	ensembl gene id	Prox1 mean RPKM	C57 mean RPKM	feature ID	fold change	FDR Pvalue	ensembl gene id	Prox1 mean RPKM	C57 mean RPKM
Col13a1	3.0	4.9E-38	ENSMUSG00000058806	21.61	5.55	Maml2	2.7	4.5E-19	ENSMUSG00000031925	16.26	4.73
Col9a2	3.0	5.4E-14	ENSMUSG00000028626	28.97	7.50	Col3a1	2.7	7.8E-04	ENSMUSG00000026043	46.23	13.96
Lpl	3.0	1.0E-25	ENSMUSG00000015568	13.47	3.52	Smim24	2.7	1.6E-03	ENSMUSG00000078439	2.92	0.86
Ldhb	3.0	2.0E-18	ENSMUSG00000030246	81.89	21.44	Stbd1	2.7	2.7E-08	ENSMUSG00000047963	6.27	1.83
Vash2	3.0	7.3E-28	ENSMUSG00000037568	25.76	6.77	Sepp1	2.7	2.3E-11	ENSMUSG00000064373	62.12	18.56
Dnm1	3.0	6.3E-04	ENSMUSG00000026825	3.74	1.00	Nupr1	2.7	2.2E-11	ENSMUSG00000030717	116.88	33.45
Col25a1	3.0	1.0E-04	ENSMUSG00000058897	2.06	0.55	Rnf165	2.7	1.9E-17	ENSMUSG00000025427	13.72	4.03
Cxcl12	3.0	2.2E-03	ENSMUSG00000061353	4.66	1.28	Sertad4	2.7	2.0E-03	ENSMUSG00000016262	3.32	0.99
Thbs2	3.0	2.9E-04	ENSMUSG00000023885	3.84	1.01	Lama4	2.7	1.6E-09	ENSMUSG00000019846	13.31	4.01
Car14	3.0	3.6E-16	ENSMUSG00000038526	35.73	9.55	Prkcb	2.7	3.0E-06	ENSMUSG00000052889	2.59	0.76
Lum	3.0	6.2E-05	ENSMUSG00000036446	75.36	20.41	Sh3pxd2a	2.7	9.7E-08	ENSMUSG00000053617	15.55	4.66
Calml3	2.9	9.9E-03	ENSMUSG00000063130	3.47	0.94	Irx5	2.6	4.8E-03	ENSMUSG00000031737	2.93	0.86
Egfr	2.9	8.0E-04	ENSMUSG00000020122	2.80	0.77	Hif3a	2.6	3.1E-10	ENSMUSG00000004328	7.63	2.26
Nes	2.9	5.1E-24	ENSMUSG00000004891	124.95	33.66	Slc1a3	2.6	3.1E-08	ENSMUSG00000005360	6.45	1.92
Cd83	2.9	5.5E-06	ENSMUSG00000015396	3.53	0.94	Creb3l2	2.6	9.4E-15	ENSMUSG00000038648	27.83	8.35
Rgma	2.9	1.8E-10	ENSMUSG00000070509	6.91	1.86	Akr1b10	2.6	1.7E-05	ENSMUSG00000061758	2.06	0.62
Mt2	2.9	3.1E-04	ENSMUSG00000031762	5.68	1.52	Ntf3	2.6	2.4E-03	ENSMUSG00000049107	3.96	1.17
Gm26917	2.9	4.8E-03	ENSMUSG00000097971	4097.06	1152.77	Fez1	2.6	2.9E-17	ENSMUSG00000032118	16.29	4.87
Dkk2	2.9	7.5E-04	ENSMUSG00000028031	24.01	6.61	Efemp1	2.6	4.1E-04	ENSMUSG00000020467	11.52	3.47
Ror2	2.9	2.2E-05	ENSMUSG00000021464	3.52	0.97	Slc9a3r1	2.6	2.7E-11	ENSMUSG00000020733	28.26	8.55
5730559C18Rik	2.9	5.6E-07	ENSMUSG00000041605	5.89	1.63	Prom1	2.6	5.3E-16	ENSMUSG00000029086	23.87	7.23
Pla2g4a	2.9	6.7E-27	ENSMUSG00000056220	7.70	2.09	Dok1	2.6	2.3E-09	ENSMUSG00000068335	8.51	2.57
2700069I18Rik	2.9	2.6E-05	ENSMUSG00000086224	3.38	0.93	Apod	2.6	7.5E-04	ENSMUSG00000022548	2.39	0.72
Mid2	2.9	5.7E-10	ENSMUSG00000000266	3.29	0.90	Dgkh	2.6	1.2E-03	ENSMUSG00000034731	2.33	0.70
Krt18	2.8	1.3E-05	ENSMUSG00000023043	21.26	6.01	Itpr3	2.6	1.8E-05	ENSMUSG00000042644	2.70	0.83
AY036118	2.8	7.7E-03	ENSMUSG00000045999	175.12	50.59	Jph2	2.6	2.1E-09	ENSMUSG00000017817	4.07	1.23
Rbm20	2.8	2.9E-08	ENSMUSG00000043639	2.16	0.60	Lingo1	2.6	8.9E-11	ENSMUSG00000049556	4.10	1.24
Bdh2	2.8	2.8E-05	ENSMUSG00000028167	10.74	3.02	Cryl1	2.6	2.4E-05	ENSMUSG00000021947	3.49	1.05
Fam101b	2.8	4.3E-20	ENSMUSG00000020846	16.16	4.52	Gm4524	2.6	1.0E-12	ENSMUSG00000090257	16.01	4.81
Chd3	2.8	1.5E-10	ENSMUSG00000018474	27.76	7.93	Mtcl1	2.6	4.2E-20	ENSMUSG00000052105	22.25	6.82
Gm14236	2.8	9.7E-03	ENSMUSG00000086411	207.37	60.61	Olfml3	2.6	1.8E-10	ENSMUSG00000027848	30.96	9.23
Mreg	2.8	8.7E-07	ENSMUSG00000039395	3.57	1.01	Crabp2	2.6	7.1E-06	ENSMUSG00000004885	99.87	30.97
Ddr2	2.8	3.0E-04	ENSMUSG00000026674	5.51	1.59	Adam19	2.6	7.0E-04	ENSMUSG00000011256	2.88	0.91
Ntrk2	2.8	3.0E-14	ENSMUSG00000055254	9.05	2.54	Anxa2	2.5	1.3E-12	ENSMUSG00000032231	33.43	10.37
Olfml1	2.8	4.2E-02	ENSMUSG00000051041	2.42	0.70	Slc6a15	2.5	8.6E-04	ENSMUSG00000019894	17.03	5.32
S100a1	2.8	1.5E-06	ENSMUSG00000044080	8.40	2.39	Clmp	2.5	3.6E-09	ENSMUSG00000032024	7.36	2.29
C230034O21Rik	2.8	3.5E-02	ENSMUSG00000086181	2.77	0.78	Sparcl1	2.5	4.5E-14	ENSMUSG00000029309	57.05	17.89
Tenm4	2.7	8.5E-05	ENSMUSG00000048078	8.47	2.46	Fbln2	2.5	8.9E-04	ENSMUSG00000064080	6.29	1.98
Dmp1	2.7	2.5E-02	ENSMUSG00000029307	22.74	6.84	Col11a1	2.5	3.3E-03	ENSMUSG00000027966	6.04	1.92
Ccdc177	2.7	2.5E-09	ENSMUSG00000062961	2.95	0.85	Paqr4	2.5	8.3E-08	ENSMUSG00000023909	6.13	1.91
Sall2	2.7	2.8E-18	ENSMUSG00000049532	43.54	12.57	Optc	2.5	3.6E-02	ENSMUSG00000010311	6.11	1.85
Gzmm	2.7	1.5E-03	ENSMUSG00000054206	2.93	0.84	Clip1	2.5	6.1E-16	ENSMUSG00000049550	12.94	4.08
Rab27a	2.7	1.8E-04	ENSMUSG00000032202	5.86	1.72	Shank1	2.5	6.7E-08	ENSMUSG00000038738	4.81	1.51
Antxr1	2.7	1.1E-24	ENSMUSG00000033420	67.56	19.41	Fzd8	2.5	1.5E-07	ENSMUSG00000036904	4.12	1.30
Twist1	2.7	1.2E-02	ENSMUSG00000035799	10.59	3.10	Trib2	2.5	1.1E-23	ENSMUSG00000020601	22.21	6.98
Cdo1	2.7	5.1E-07	ENSMUSG00000033022	12.86	3.72						